Tokyo, Japan) and *Ex Taq* DNA polymerase with 3' exonuclease activity (TaKaRa Bio Inc.). The PCR products were purified and used as templates for cycle sequencing reactions with the Big Dye Terminator Cycle Sequencing Kit (version 1.0; Applied Biosystems). The mutations found in a PCR product were verified by reverse sequencing and then were reconfirmed in two independently amplified PCR products.

2.5. Statistical analysis

Statistical analyses were performed using the SAS software package (version 9.0; SAS Institute, Cary, NC). Student's *t*-test was used to compare the average ages of the patients. The chi-square test and Fisher's exact test were used to examine relationships between categoric variables and the genetic markers.

Due to the similar genetic backgrounds, as determined by a univariate analysis, distal and rectal cancers were combined. Logistic regression models were used to estimate the multivariable relationship between the alternations of these genetic markers and the odds of tumor locations. Initial logistic regression models examined the main effects only. Interactions between these factors were explored in subsequent logistic models. All reported *P* values were two-sided, and $P < 0.05$ was considered statistically significant.

3. Results

The clinicopathologic backgrounds of the tumors used in this study are shown in Table 1. The four key genetic factors induced in the current study have all been well documented, though they are seldom studied in the same large panel. The MSI, DNA aneuploidy, *TP53* gene mutation, and *TP53* LOH were detected in 14.4, 73.3, 36.1, and 59.4% percent of cases, respectively, and these findings did not differ from those reported in Caucasians.

The association between genetic features and clinicopathologic variables are shown in Table 2. The genetic factors were not associated with age, gender, pathologic gross type, tumor stage, or lymphatic invasion. The tumor location was found to be significantly associated with all the four markers studied. Moreover, MSI was associated with a lower degree of differentiation and less frequent

Table 2
Genetic features and clinicopathologic variables in CRC

	MSI			DNA index			*TP53* gene			*TP53* LOH[h]		
Factors	MSI(−)	MSI(+)	*P*	Diploidy	Aneuploidy	*P*	WT[f]	Mut[g]	*P*	LOH(−)	LOH(+)	*P*
Age (mean)	64.4	65.7	0.585	65.0	64.4	0.758	63.6	66.3	0.124	65.9	63.8	0.289
Gender												
Male	89	15	0.992	26	78	0.555	64	40	0.442	29	63	0.710
Female	65	11		22	54		51	25		23	44	
Location												
Proximal colon	41	18	<0.001	23	36	0.034	45	14	0.047	24	28	0.045
Distal colon	44	5		11	38		29	20		11	30	
Rectum	69	3		14	58		41	31		17	49	
Gross												
Polypoid	135	21	0.360	39	117	0.211	96	60	0.082	43	94	0.384
Flat	19	5		9	15		19	5		9	13	
Histologic grade												
Grade 1[a]	76	11	<0.001	26	61	0.440	58	29	<0.001	28	50	0.509
Grade 2[b]	65	5		15	55		36	34		16	43	
Grade 3[c]	13	10		7	16		21	2		8	14	
TNM stage												
I–II	67	14	0.328	27	54	0.068	55	26	0.310	25	46	0.545
III–IV	87	12		21	78		60	39		27	61	
Lymphocyte infiltration[d]												
Not prominent	70	19	0.006	31	58	0.005	60	29	0.265	31	49	0.073
Prominent	80	6		14	72		51	35		19	56	
Lymphatic invasion[e]												
None	91	15	0.835	29	77	0.726	66	40	0.682	31	64	0.961
Present	61	11		18	54		47	25		20	42	

P values showing statistical significance are underlined.
[a] Well differentiated.
[b] Moderately differentiated.
[c] Poorly differentiated or undifferentiated.
[d] Five missing data.
[e] Two missing data.
[f] *TP53* wild type.
[g] *TP53* mutation.
[h] 21 cases were not informative for *TP53* LOH estimation.

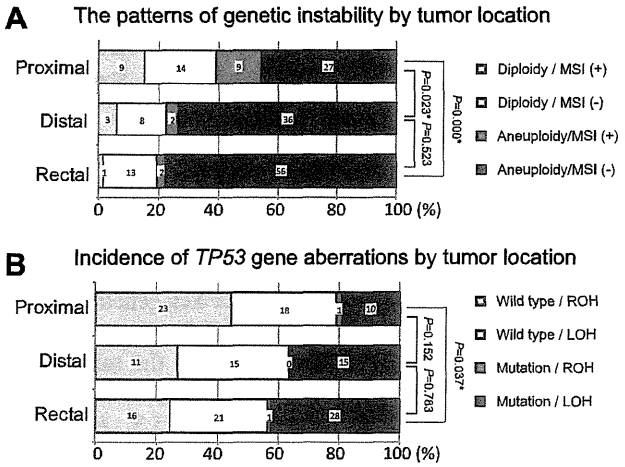

Fig. 1. The location-related genetic differences of CRC. MSI (+), high-frequency microsatellite instability; MSI (−), low-frequency microsatellite instability and microsatellite stability; WT, *TP53* wild type; Mut, mutated *TP53*; LOH (−), retention of heterozygosity; LOH (+), loss of heterozygosity. *A total of 11 cases were not informative for LOH estimation and thus were treated as missing data for the analysis. (A) Schematic illustration of the genetic instability patterns by tumor location. (B) Incidence of*TP53* gene aberrations by tumor location.

lymphocyte infiltration, which is inconsistent with previous reports [21]. The *TP53* mutations were associated with higher histologic grade, and the *TP53* LOH tended to be associated with lymphocyte infiltration.

The patterns of genomic instability were schematized according to DNA ploidy and MSI by tumor locations (Fig. 1A). The aneuploidy/MSI (−) and diploidy/MSI (+) suggested the classic CIN and MSI tumorigenesis pathways. The patterns of genetic instability were distinct in proximal colon cancers.

The integration of the *TP53* mutation and LOH was compared by tumor locations (Fig. 1B). The incidences of mutation and LOH were significantly different between the proximal colon cancer and the cancers from other parts of the colon and rectum. The tumor location showed no statistical association with either the *TP53* mutational spectra or special amino acid changes (data not shown).

The four genetic factors were associated with each other on the basis of the chi square test findings (Table 3). An acquired logistic fit model was applied successively to analyze the association between tumor location and genetic features (Table 4). The tumor location was inducted as the outcome variable, and genetic features as the explanatory variables. According to the similar genetic features of the distal colon and rectal cancers, they were combined into one group for analysis. MSI was the only parameter independently associated with tumor location ($P = 0.001$). The logistic models considered the interactions between the factors and revealed an identical result, thus only the model considered to be the main effect was shown.

To further demonstrate the involvement of MSI to tumor site–related differences, the 26 MSI (+) tumors were excluded, and then the associations were re-analyzed (Table 5, A and B). As expected, the associations between the clinicopathologic variables and DI, *TP53* mutation, and LOH vanished.

4. Discussion

It is crucial to determine whether the tumor location defines distinct genetic features of CRC because of its potential significance in both the clinical and research fields [22]. In this study, four genetic markers — MSI, DI, *TP53* mutation, and LOH — were investigated in a series of Japanese CRC to analyze whether any association exists between the tumor location and these crucial genetic markers.

The aberrations of these factors were inconsistent with most previous studies in Caucasians, despite the reported ethical difference of the CRC genetics [23]. The proximal subsets of colon cancer manifested distinct features in the genetic factors studied; i.e., less DI alternation, high MSI, low *TP53* mutation, and LOH. In addition, from a histopathological standpoint, the proximal colon cancers were prone to be poorly differentiated and less prominent in lymphocyte infiltration (data not shown), which is inconsistent with a previous study [24]. The distal colon cancer and rectal cancer shared similar genetic and biologic features.

Intriguingly, the multivariate analysis indicated that MSI was the only factor significantly associated with tumor

Table 3
Genetic features of sporadic CRC

		MSI			DNA index			*TP53* gene		
Factors		MSI (−)	MSI (+)	*P*	Diploidy	Aneuploidy	*P*	WT	Mut	*P*
DNA index	Diploidy	35	13	0.006						
	Aneuploidy	119	13							
TP53 gene	WT[a]	90	25	<0.001	47	68	<0.001			
	Mut[b]	64	1		1	64				
TP53 LOH	LOH(-)	37	15	0.004	40	12	<0.001	50	2	<0.001
	LOH(+)	96	11		2	105		54	53	

P values showing statistical significance are underlined.
[a] *TP53* wild type.
[b] *TP53* mutation.

Table 4
Logistic regression analysis of genetic factors and the distal versus proximal localization of CRC

	Object	Control	Odds ratio	95% CI[c]	*P*
CIN[a]	Aneuploidy	Diploidy	1.437	0.326–6.334	0.632
MSI[b]	MSI (−)	MSI (+)	5.052	1.915–13.325	0.001
TP53 LOH	LOH	ROH	1.701	0.401–7.217	0.471
TP53 mutation	Mutation	Wild type	1.170	0.480–2.848	0.730

P value showing statistical significance is underlined.
[a] Chromosomal instability.
[b] Microsatellite instability.
[c] 95% confidence interval.

location, which was similar to a previous report on colon cancer in a Caucasian population [14]. This report estimated the p53 changes by immunohistochemical staining, and MSI were studied by a denaturing gel electrophoresis–autoradiograph assay, which is supposed to have unavoidable technological problems [25].

In the current study, MSI and LOH were studied by an accurate fragment analysis [15], and the *TP53* mutation was evaluated by direct sequencing. The DI was detected by LSC, a methodology that enables a direct morphologic evaluation of the cell population. Furthermore, when MSI-H tumors were excluded, the associations between the pathologic variables and the genetic features disappeared. The analysis strongly indicated that the location-related differences of CRC were caused by the inclusion of MSI-H tumors.

The MSI phenotype is a derived genetic or epigenetic defect in the DNA mismatch repair machinery, which plays a crucial role in DNA metabolism and cell cycle control [26]. The MSI defines a tumorigenesis pathway characterized by an elevated mutation rate in simple-repeat nucleotides independent of CIN. The less frequent DI aberrations in the proximal colon could be explained by the inclusion of the MSI tumors. MSI tumors comprise

Table 5A
Genetic features and clinicopathologic factors in MSI (+) tumors

	DNA index			*TP53* gene			*TP53* LOH[h]		
Factors	Euploidy	Aneuploidy	*P*	WT[f]	Mut[g]	*P*	LOH(−)	LOH(+)	*P*
Age (mean)	66.0	63.2	0.478	64.3	66.6	0.665	65.0	64.1	0.819
Gender									
Male	12	15	0.228	22	5	0.695	14	13	0.485
Female	13	8		18	3		13	8	
Location									
Proximal	16	12	0.489	25	3	0.415	17	11	0.302
Distal	5	4		7	2		6	3	
Rectal	4	7		8	3		4	7	
Gross									
Polypoid	2	4	0.326	6	0	0.242	2	4	0.226
Flat	23	19		34	8		25	17	
Histologic grade									
Grade 1[a]	11	12	0.321	17	6	0.233	12	11	0.531
Grade 2[b]	9	4		12	1		9	4	
Grade 3[c]	5	7		11	1		6	6	
pStage									
I–II	16	11	0.259	22	5	0.696	17	10	0.288
III–IV	9	12		18	3		10	11	
Lymphocyte infiltration[d]									
Negative	18	13	0.113	26	5	1.000	20	11	0.063
Positive	5	10		12	3		5	10	
Lymphatic invasion[e]									
None	14	16	0.422	24	6	0.46	15	15	0.375
Present	10	7		15	2		11	6	

[a] Well differentiated.
[b] Moderately differentiated.
[c] Poorly differentiated or undifferentiated.
[d] Two missing data.
[e] One missing data.
[f] *TP53* wild type.
[g] *TP53* mutation.
[h] A total of 21 cases were not informative for *TP53* LOH estimation.

Table 5B
Genetic features and clinicopathologic variables in MSI (−) tumors

	DNA index			*TP53* gene			*TP53* LOH[h]		
Factors	Diploidy	Aneuploidy	*P*	WT[f]	Mut[g]	*P*	LOH(−)	LOH(+)	*P*
Age (mean)	63.6	64.6	0.629	63.0	66.4	0.053	65.6	68.3	0.388
Gender									
Male	19	70	0.634	49	40	0.318	20	57	0.578
Female	16	49		41	24		17	39	
Location									
Proximal colon	14	27	0.140	28	13	0.320	14	20	0.115
Distal colon	8	36		24	20		7	29	
Rectum	13	56		38	31		16	47	
Gross									
Polypoid	28	107	0.135	76	59	0.140	30	86	0.203
Flat	7	12		14	5		7	10	
Histologic grade									
Grade 1[a]	21	55	0.312	48	28	0.191	22	45	0.418
Grade 2[b]	11	54		31	34		12	42	
Grade 3[c]	3	10		11	2		3	9	
TNM stage									
I–II	19	48	0.102	42	25	0.220	16	41	0.956
III–IV	16	71		48	39		21	55	
Lymphocyte infiltration[d]									
Not prominent	20	50	0.069	42	28	0.642	18	43	0.664
Prominent	13	67		45	35		18	51	
Lymphatic invasion[e]									
None	22	69	0.511	52	39	0.819	23	57	0.683
Present	12	49		36	25		13	38	

[a] Well differentiated.
[b] Moderately differentiated.
[c] Poorly differentiated or undifferentiated.
[d] Five missing data.
[e] Two missing data.
[f] *TP53* wild type.
[g] *TP53* mutation.
[h] A total of 21 cases were not informative for *TP53* LOH estimation.

a pathologically and clinically distinct subtype of CRC, which tend to occur in the proximal subset of the colon, and show poor differentiation, mucin production, and Crohn's-like peritumoral lymphoid response [27].

In CRC, MSI is exclusive to the *TP53* mutation, which indicates a distinct tumorigenesis pathway independent of the defects in the p53-related pathways. The MSS and MSI-L were similar in *TP53* aberrations and DI alternations (data not shown), thus suggesting a similar, if not identical, tumorigenesis background. Therefore, they were combined as MSI (−). The proximal accumulation of MSI tumors might thus demonstrate a relatively low incidence of *TP53* aberrations.

The prognostic value and clinical application of MSI as a chemosensitivity indicator still remains controversial [28]. To some extent, the diversity of the biologic significance of the MSI phenotype might be attributed to the lack of a standardized methodology for MSI detection [29]. MSI is implied as a favorable prognostic factor, according to a detailed review of 2006 ASCO [30]. Another report concluded that *TP53* mutations in proximal tumors are associated with a significantly worse survival, based on a univariate analysis, but the significance was diminished by a multivariate analysis when other factors, including MSI, were considered [31]. The current results can explain such a finding; i.e., the favorable prognosis of the *TP53* wild type tumors in the proximal subset of the colon were probably accounted for by the MSI-H tumors, which have a better prognosis and are possibly *TP53* wild type. Similarly, another study suggests that *TP53* mutations, when considered with tumor sites, are associated with a poor prognosis [12]. MSI, however, was not considered in that study. The different prognosis effects of *TP53* mutation by tumors locations may be partly derived from the inclusion of MSI-H tumors. Therefore, MSI is a molecular marker that can provide valuable information in colon cancer patients. In the appropriate clinical setting, MSI data can be used in clinical decision-making. Specifically, the favorable outcome of stage II colon cancers with MSI indicates that such patients should not receive adjuvant chemotherapy.

The mutational events of some important oncogene/tumor suppressor genes such as *KRAS*, *APC*, *PIK3CA*, and *BRAF* were also studied. The alternations of these genes did not show any obvious location-related differences, so they were not documented. These indicated that

the lower digestive tract cancers share significant genetic features, however, despite the location-related differences that are emphasized in this study.

To sum up, proximal colon cancers were genetically distinct from distal colon cancers and rectal cancers; the rectal cancers and distal colon cancers share similar genetic profiles. Importantly, MSI was the major and only factor associated with the CRC site–related genetic and clinicopathologic differences. MSI (−) tumors had similar genetic profiles, regardless of the tumor locations. This study proposes that site-related differences in CRC might be attributable to the inclusion of MSI tumors. These findings support the idea that MSI indicates a unique category of CRC. The current study strongly implies that the MSI status, instead of the tumor location, should thus be a major concern in the understanding of CRC.

Acknowledgments

We are grateful to Drs. Kitao Hiroyuki, Sugiyama Masahiko, and Yamashita Natsumi for helpful discussions. We also thank Dr. Brian Quinn for critical comments on the manuscript.

References

[1] Minami Y, Nishino Y, Tsubono Y, Tsuji I, Hisamichi S. Increase of colon and rectal cancer incidence rates in Japan: trends in incidence rates in Miyagi Prefecture, 1959–1997. J Epidemiol 2006;16:240–8.

[2] Yiu HY, Whittemore AS, Shibata A. Increasing colorectal cancer incidence rates in Japan. Int J Cancer 2004;109:777–81.

[3] Stang A, Stabenow R, Stegmaier C, Eisinger B, Bischof-Hammes E, Jockel KH. Unexplained inversion of the incidence ratio of colon and rectal cancer among men in East Germany. A time trend analysis including 147,790 cases. Eur J Epidemiol 2007;22:245–55.

[4] Bufill JA. Colorectal cancer: evidence for distinct genetic categories based on proximal or distal tumor location. Ann Intern Med 1990; 113:779–88.

[5] Loeb LA. A mutator phenotype in cancer. Cancer Res 2001;61:3230–9.

[6] Lengauer C, Kinzler KW, Vogelstein B. Genetic instabilities in human cancers. Nature 1998;396:643–9.

[7] Walther A, Houlston R, Tomlinson I. Association between chromosomal instability and prognosis in colorectal cancer: a meta-analysis. Gut 2008;57:941–50.

[8] Boyer JC, Umar A, Risinger JI, Lipford JR, Kane M, Yin S, Barrett JC, Kolodner RD, Kunkel TA. Microsatellite instability, mismatch repair deficiency, and genetic defects in human cancer cell lines. Cancer Res 1995;55:6063–70.

[9] Pellman D. Cell biology: Aneuploidy and cancer. Nature 2007;446: 38–9.

[10] Miyazaki M, Furuya T, Shiraki A, Sato T, Oga A, Sasaki K. The relationship of DNA ploidy to chromosomal instability in primary human colorectal cancers. Cancer Res 1999;59:5283–5.

[11] Vogelstein B, Lane D, Levine AJ. Surfing the p53 network. Nature 2000;408:307–10.

[12] Russo A, Bazan V, Iacopetta B, Kerr D, Soussi T, Gebbia N. The TP53 colorectal cancer international collaborative study on the prognostic and predictive significance of p53 mutation: influence of tumor site, type of mutation, and adjuvant treatment. J Clin Oncol 2005;23:7518–28.

[13] Knudson AG Jr. Mutation and cancer: statistical study of retinoblastoma. Proc Natl Acad Sci USA 1971;68:820–3.

[14] Sinicrope FA, Rego RL, Foster N, Sargent DJ, Windschitl HE, Burgart LJ, Witzig TE, Thibodeau SN. Microsatellite instability accounts for tumor site-related differences in clinicopathologic variables and prognosis in human colon cancers. Am J Gastroenterol 2006;101:2818–25.

[15] Oda S, Oki E, Maehara Y, Sugimachi K. Precise assessment of microsatellite instability using high resolution fluorescent microsatellite analysis. Nucleic Acids Res 1997;25:3415–20.

[16] Boland CR, Thibodeau SN, Hamilton SR, Sidransky D, Eshleman JR, Burt RW, Meltzer SJ, Rodriguez-Bigas MA, Fodde R, Ranzani GN, Srivastava S. A National Cancer Institute Workshop on Microsatellite Instability for cancer detection and familial predisposition: development of international criteria for the determination of microsatellite instability in colorectal cancer. Cancer Res 1998;58:5248–57.

[17] Yoshino I, Osoegawa A, Yohena T, Kameyama T, Oki E, Oda S, Maehara Y. Loss of heterozygosity (LOH) in non-small cell lung cancer: difference between adenocarcinoma and squamous cell carcinoma. Respiratory medicine 2005;99:308–12.

[18] Sasaki K, Kurose A, Miura Y, Sato T, Ikeda E. DNA ploidy analysis by laser scanning cytometry (LSC) in colorectal cancers and comparison with flow cytometry. Cytometry 1996;23:106–9.

[19] Hiddemann W, Schumann J, Andreef M, Barlogie B, Herman CJ, Leif RC, Mayall BH, Murphy RF, Sandberg AA. Convention on nomenclature for DNA cytometry. Cancer Genet Cytogenet 1984;13:181–3.

[20] Yamamoto Y, Matsuyama H, Chochi Y, Okuda M, Kawauchi S, Inoue R, Furuya T, Oga A, Naito K, Sasaki K. Overexpression of BUBR1 is associated with chromosomal instability in bladder cancer. Cancer Genet Cytogenet 2007;174:42–7.

[21] Jass JR. HNPCC and Sporadic MSI-H Colorectal cancer: a review of the morphological similarities and differences. Fam Cancer 2004;3: 93–100.

[22] Gervaz P, Bucher P, Morel P. Two colons-two cancers: paradigm shift and clinical implications. J Surg Oncol 2004;88:261–6.

[23] Saltzstein SL, Behling CA. Age and time as factors in the left-to-right shift of the subsite of colorectal adenocarcinoma: a study of 213,383 cases from the California Cancer Registry. J Clin Gastroenterol 2007; 41:173–7.

[24] Iacopetta B. Are there two sides to colorectal cancer? Int J Cancer 2002;101:403–8.

[25] Oda S, Maehara Y, Sumiyoshi Y, Sugimachi K. Microsatellite instability in cancer: what problems remain unanswered? Surgery 2002; 131:S55–62.

[26] Seifert M, Reichrath J. The role of the human DNA mismatch repair gene hMSH2 in DNA repair, cell cycle control and apoptosis: implications for pathogenesis, progression and therapy of cancer. J Mol Histol 2006;37:301–7.

[27] Ward R, Meagher A, Tomlinson I, O'Connor T, Norrie M, Wu R, Hawkins N. Microsatellite instability and the clinicopathological features of sporadic colorectal cancer. Gut 2001;48:821–9.

[28] Benatti P, Gafa R, Barana D, Marino M, Scarselli A, Pedroni M, Maestri I, Guerzoni L, Roncucci L, Menigatti M, Roncari B, Maffei S, Rossi G, Ponti G, Santini A, Losi L, Di Gregorio C, Oliani C, Ponz de Leon M, Lanza G. Microsatellite instability and colorectal cancer prognosis. Clin Cancer Res 2005;11:8332–40.

[29] Söreide K, Janssen EAM, Söiland H, Körner H, Baak JPA. Microsatellite instability in colorectal cancer. Br J Surg 2006;93:395–406.

[30] Locker GY, Hamilton S, Harris J, Jessup JM, Kemeny N, Macdonald JS, Somerfield MR, Hayes DF, Bast RC Jr. A.S.C.O. 2006 update of recommendations for the use of tumor markers in gastrointestinal cancer. J Clin Oncol 2006;24:5313–27.

[31] Samowitz WS, Curtin K, Ma K-n, Edwards S, Schaffer D, Leppert MF, Slattery ML. Prognostic significance of *p53* mutations in colon cancer at the population level. Int J Cancer 2002;99:597–602.

Cancer Science
The official journal of the Japanese Cancer Association JCA

High expression of BUBR1 is one of the factors for inducing DNA aneuploidy and progression in gastric cancer

Koji Ando,[1] Yosihiro Kakeji,[1,4] Hiroyuki Kitao,[2] Makoto Iimori,[2] Yan Zhao,[1] Rintaro Yoshida,[1] Eiji Oki,[3] Keiji Yoshinaga,[1] Takuya Matumoto,[1] Masaru Morita,[1] Yoshihisa Sakaguchi[3] and Yoshihiko Maehara[1]

Departments of [1]Surgery and Science, [2]Molecular Oncology, Graduate School of Medical Sciences, Kyushu University and [3]National Kyushu Cancer Center, Fukuoka, Japan

(Received September 24, 2009/Revised November 23, 2009/Accepted November 24, 2009/Online publication February 2, 2010)

Gastric cancers show high frequency of DNA aneuploidy, a phenotype of chromosomal instability. It is suggested that the abnormal spindle assembly checkpoint is involved in DNA aneuploidy, but the underlying mechanism is still unclear. We studied the mechanism by assessing the expression of BUBR1 in gastric cancer. The DNA ploidy patterns of 116 gastric cancer samples obtained from the Department of Surgery and Science at Kyushu University Hospital were analyzed. Of those, DNA aneuploidy was seen in 70 (60.3%) cases of gastric cancer. The expression of BUBR1 was studied by immunohistochemistry in 181 gastric cancer samples and by real-time RT-PCR in several gastric cancer cell lines. Ninety-one (50.3%) cases had high expression of BUBR1 and those cases correlated significantly with DNA aneuploidy ($P < 0.05$). Also high expression of BUBR1 cases had significant correlation with deep invasion, lymph node metastasis, liver metastasis, and poor prognosis. In gastric cancer cell lines, high expression of BUBR1 had a significant relationship with DNA aneuploidy ($P < 0.05$). Then, gastric cancer cell lines MKN-28 and SNU-1 were transfected with full-length BUBR1 to observe the significance of the change in BUBR1 expression. Enforced expression of BUBR1 resulted in changes to the ploidy pattern and high Ki-67 expression. Collectively, our clinical and *in vitro* data indicate that high expression of BUBR1 may be one of causative factors for the induction of DNA aneuploidy and progression of gastric cancer. (*Cancer Sci* 2010; 101: 639–645)

DNA aneuploidy is a state of cells with an abnormal number of chromosomes. More than a century ago, David Paul Hansemann observed that cancer cells have abnormal chromosome numbers.[1] In 1997, Lengauer *et al.* reported that DNA aneuploidy was seen in 85% of colorectal cancers.[2] This form of chromosomal instability reflected a continuing cellular defect that persisted throughout the lifetime of the cancer cell and was independent from microsatellite instability which was a recessive trait. DNA aneuploidy is an important phenomenon for cancer cells; however, whether or not DNA aneuploidy may be a cause for carcinogenesis is still controversial. To date many analyses have focused on DNA aneuploidy and it is now known that mutation or inactivation in p53, 'the guardian of genome', results in DNA aneuploidy.[3,4]

Recently, it has been defined that DNA aneuploidy occurs due to disorders in the spindle assembly checkpoint.[5] This checkpoint is the mechanism which delays the separation of sister chromatids until all the kinetochores of chromosomes are correctly attached to the spindle.[6] It has been reported that knockdown or overexpression of spindle assembly checkpoint molecules resulted in DNA aneuploidy and carcinogenesis in mice.[7] The disorders in spindle assembly checkpoint molecules may be involved in DNA aneuploidy and carcinogenesis in humans.

BUBR1 kinase, a member of the BUB (budding uninhibited by benzimidazole) gene family, is one of the key molecules in the spindle assembly checkpoint. It accumulates on the unattached kinetochore.[8] BUBR1 targets Cdc20, an APC/C (anaphase promoting complex/cyclosome; E3 ubiquitin ligase) activator, and prevents the premature onset of anaphase.[9,10] The degradation of Cdc20 represents a critical control mechanism ensuring the inactivation of APC/C in response to the spindle assembly checkpoint.[11] In addition, BUBR1 independently interacts with securin.[12] Matsuura *et al.* reported that a mutation in the *BUBR1* gene is detected in premature chromatid separation (PCS) syndrome, which has been often associated with chromosomal instability and malignancies. Furthermore, an abnormal spindle assembly checkpoint was observed in this syndrome.[13,14]

Although mutations of BUBR1 have been rarely observed in clinical samples,[15,16] high expression of BUBR1 has often been reported in several malignancies and correlated with chromosomal instability,[17–19] but not thus far in gastric cancer.

Herein, we report the significance of DNA aneuploidy and BUBR1 high expression in gastric cancer by analyzing gastric cancer clinical samples and cell lines.

Material and Methods

Patients studied. This study included 181 unselected Japanese patients with primary gastric cancer, all of whom underwent a gastrectomy between 1994 and 2006 at the Department of Surgery and Science, Graduate School of Medical Sciences, Kyushu University Hospital, Fukuoka. They included 121 men and 60 women, ranging in age from 29 to 90 years (mean, 64.2 years). In each case, a careful informed consent was obtained. Those who refused were not included. A thorough histological examination was made by using H&E-stained tissue preparations, and the histological classification was made according to the general rules set up by the Japanese Gastric Cancer Association.[20] No patient treated preoperatively with cytotoxic drugs was included in this study.

Immunohistochemical staining of BUBR1. Formalin-fixed, paraffin-embedded tissue specimens were used for immunohistochemical staining. A paraffin block which contained both cancerous tissue, invading the deepest area of the stomach wall, and adjacent noncancerous tissue, was used in each case. Immunohistochemical staining was done as described in previous reports.[19,21,22] Briefly, the sections were pretreated with

[4]To whom correspondence should be addressed.
E-mail: kakeji@surg2.med.kyushu-u.ac.jp

doi: 10.1111/j.1349-7006.2009.01457.x

autoclaving (121°C) for 15 min in 0.01 mol/L citrate-buffered saline (pH 6.0) for antigen retrieval. Endogenous peroxidase activity was blocked by incubation with 0.3% H_2O_2 for 10 min. The sections were incubated with mouse monoclonal antibodies against BUBR1 (Clone 9, 1:100; BD Transduction Laboratories, San Jose, CA, USA) at 4°C overnight. Streptavidin–biotin complex and horseradish peroxidase were applied, and the reaction products were visualized using the Histofine SAB-PO (M) immunohistochemical staining kit (Nichirei, Tokyo, Japan), according to the manufacturer's instructions. Two blinded observers (K.A. and Y.Z.) independently examined immunostained sections. The intensity of cytoplasmic staining of BUBR1 was scored on a three-point scale in comparison to the staining of lymph follicles which were equally stained in all 181 specimens. Weaker staining was scored 0, and similar and stronger than the follicle were scored 1 and 2, respectively.

Analysis for DNA ploidy. Nuclear DNA content was measured by using laser scanning cytometry (LSC; CompuCyte, Westwood, MA, USA) as described previously.[23,24] The same paraffin-embedded blocks that were used for immunohistochemical staining were used for this analysis. A DNA content histogram was generated and DNA ploidy was determined. DNA index (DI) was calculated according to previously published principles.[25,26] For every case, the nuclei were observed after each scan to exclude debris and attached nuclei from the analysis. The DI of G0/G1-phase lymphocyte or fibroblasts were used as a reference of DI = 1.0. Tumors with a DI < 1.2 were defined as diploid; DI ≧ 1.2 or multi-indexed samples were defined as aneuploid.

High-resolution fluorescent microsatellite analysis (HRFMA) for MSI. HRFMA has been described in detail elsewhere.[27] Briefly, genomic DNA isolated from cancerous and corresponding noncancerous tissue specimens was used to amplify microsatellite loci by polymerase chain reaction (PCR) using primer sets labeled with a fluorescent compound, ROX (6-carboxy-x-rhodamine) or HEX (6-carboxy-20,40,70,4,7,-hexachlorofluorescein). The fluorescently labeled PCR products were mixed, denatured, and loaded onto an ABI 310 sequencer (Applied Biosystems, Foster City, CA, USA) for fragment analysis. The data were processed using the GeneScan software package (Applied Biosystems). An alternation in the length of a microsatellite PCR fragment from cancerous tissues was defined as MSI positive. According to the guidelines established by the National Cancer Institute (NCI), MSI was defined by the frequency of positive findings of five reference markers: D2S123, D5S107, D10S197, D11S904, D13S175.[28] MSI status was classified as follows: microsatellite instability high (MSI-H), >30% of loci demonstrate MSI; microsatellite instability low, ≤30% of loci demonstrate MSI; and microsatellite stability, no positive MSI detected in any of the loci. MSI-H was labeled 'MSI (+)' and the rest 'MSI (–)'.

TP53 gene mutation analysis. The *TP53* gene exon 5 to exon 9 including exon–intron junctions were amplified by PCR using p53 primers (Nippon Gene, Tokyo, Japan) and *Ex Taq* DNA polymerase with 3′ exonuclease activity (Takara Bio, Tokyo, Japan). The PCR products were purified and used as templates for cycle-sequencing reactions with the Big Dye Terminator Cycle Sequencing Kit version 1 (Applied Biosystems). Mutations found in a PCR product were verified by reverse sequencing and reconfirmed in two independently amplified PCR products.

Gastric cancer cell lines and cell culture. Human gastric cancer cell lines MKN-28 (JCRB0253), MKN-74 (JCRB0255), SNU-1 (CRL-5971), SNU-16 (CRL-5974), NUGC-4 (JCRB0834), KATO III (JCRB0611), NCI-N87 (CRL-5822), and human fibroblast MRC-5 (CCL-171) were grown in monolayer cultures in RPMI-1640 supplemented with fetal bovine serum (10% v/v) and glutamine (2 mM) at 37°C in a 5% CO_2 environment. MKN-28, MKN-74, NUGC-4, and KATO III were obtained from the Japanese Cancer Research Resource Bank (JCRB). SNU-1, SNU-16, NCI-N87, and MRC-5 were obtained from ATCC (Manassas, VA, USA). In this experiment, cell lines were used between passage 3 and passage 6.

Analysis for DNA ploidy in gastric cancer cell lines. Each of the cell lines were incubated in four-well chamber slide glasses. MRC-5 was grown in one of the chambers as a normal control. When they reached 80% confluence, generally after 3 days, the media were changed to serum-free medium for serum starvation.[29] After 48 h of serum starvation, the slides were fixed in 70% ethanol and stained with propidium iodide (PI) (25μg/mL) including RNaseA (10 mg/mL). DNA ploidy was analyzed in LSC. The DNA index of the G0/G1 phase of MRC-5 (normal human fibroblast cell line) was used as reference of DI = 1.0. Cell lines with a DI < 1.2 were defined as diploid; DI ≧ 1.2 or multi-indexed cell lines were defined as aneuploid.

Quantification of the mRNA of gastric cancer cell lines using real-time quantitative RT-PCR. The pellets of each of the gastric cancer cell lines were homogenized. Total RNA was isolated using an RNeasy mini kit (Qiagen, Chatsworth, CA, USA) according to the manufacturer's instructions. cDNA was synthesized with random hexamer primers and Superscript III reverse transcriptase according to manufacturer's instructions and the product was used for further analysis. BUBR1 transcription was quantified using the LightCycler (Roche Molecular Biochemicals, Mannheim, Germany) PCR protocol, in which fluorescence emission is attributable to binding of SYBR Green I dye to amplified products and can be detected and measured essentially. The relative quantitation value is expressed as 2–Ct, where Ct is the difference between the mean Ct value of triplicates of the sample and of the endogenous β-actin control. The primer sequences for Real-time RT-PCR were as follows: BUBR1, 5′-CTCGTGGCAATACAGCTTCA-3′ (forward) and 5′-CTGGTCAATAGCTCGGCTTC-3′ (reverse);[30] Ki-67, 5′-ACTTGCCTCCTAATACGCC-3′ (forward) and 5′-TTACTACATCTGCCCATGA-3′ (reverse);[31] and β-actin, 5′-CCACGAAACTACCTTCAAC-3′ (forward) and 5′-GATCTTCATTGTGCTGGG-3′ (reverse).

BUBR1 transfection to MKN-28 and SNU-1. Gastric cancer cell lines MKN-28 and SNU-1 were transfected with pcDNA3.1 + BUBR1 or pcDNA3.1 + vector alone using FuGene HD (Roche Diagnostics, Indianapolis, IN, USA) as a transfection vehicle. The transfectants (MKN-28 Mock, MKN-28 BUBR1, SNU-1 Mock, and SNU-1 BUBR1) were selected by addition of G418 (200 μg/mL) to the culture medium.

Western blotting. Cells were lysed in a sodium dodecyl sulfate (SDS)-sample buffer containing 10% glycerol, 5% β-mercaptoethanol, 2.3% SDS, and 62.5 mM Tris-HCl (pH6.8). Ten μg of protein was analysed by SDS-PAGE followed by Western blotting. The protein blots were first probed with a mouse anti-BUBR1 (Clone 9, 1:1000; BD Transduction Laboratories) antibody or a mouse anti-β-actin (Clone AC-15, 1:2000; Sigma-Aldrich, St. Louis, MO, USA) antibody, and then with a goat-antimouse IgG conjugated with horseradish peroxidase. The specific signals on the blot were detected by the enhanced chemiluminescent method.

Growth curve assay. MKN-28 Mock and MKN-28 BUBR1 were plated in triplicate at a density of 1×10^5 cells per dish in 6-cm culture dishes. At the indicated time points after plating, cells were trypsinized, stained with Trypan blue, and the number of viable cells was directly scored by using the hemocytometer.

Statistical analysis. The statistical analysis was performed by using the JMP 6.0 statistical software package (SAS Institute, Cary, NC, USA). The Student's *t*-test, the χ^2-test, Fisher's exact test, and ANOVA one-way test were used where appropriate. The Kaplan–Meier analysis was used for overall survival.

doi: 10.1111/j.1349-7006.2009.01457.x

Results

DNA ploidy in gastric cancer. The DNA ploidy patterns of 116 gastric cancer patients were analyzed by LSC. Of those, 70 (60.3%) showed DNA aneuploidy, which was consistent with a previous report.[32]

As is shown in Table 1, DNA aneuploid tumors were significantly correlated with differentiated tumors ($P < 0.01$). This result was consistent with a previous report on DNA ploidy in gastric cancer.[33] In this study, we defined papillary and tubular adenocarcinoma as differentiated tumors and poorly differentiated adenocarcinoma and signet-ring cell carcinoma as undifferentiated tumors.[20] Mucinous carcinoma was included in undifferentiated tumors. Also, DNA aneuploid tumors had more positive vascular involvement than diploid tumors ($P < 0.05$). *TP53* gene mutation and MSI statuses were also analyzed in the same gastric cancer samples. *TP53* gene mutation was analyzed in 84 patients and 20 (23.8%) had mutations. MSI status was analyzed in 116 patients and 12 (10.3%) were MSI (+). DNA aneuploidy significantly correlated with *TP53* gene mutation ($P < 0.05$), whereas MSI (+), a maker for microsatellite stability, was reversely correlated ($P < 0.05$; Table 2).

High expression of BUBR1 in gastric cancer correlated with malignant features in gastric cancer. Abnormal spindle assembly checkpoint is suggested to be one of the major causes for DNA aneuploidy.[34] BUBR1 is one of the factors in this checkpoint and its high expression is predicted to correlate with DNA aneuploidy.[18,19] Therefore, BUBR1 expression was investigated by immunohistochemistry in 181 gastric cancer samples. The BUBR1 was mainly expressed in the cytoplasm in the tumor cells (Fig. 1). In the normal gastric epithelium, BUBR1 was expressed only in the mitosis (Fig. 1a, arrow pointed cells). This was seen in all 181 cases. These cells whose intensity of staining was similar to the lymph follicle were scored 1 (Fig. 1b); this was used as the inner control. Based on BUBR1 expression in the normal gastric epithelium which was scored 1, BUBR1 was considered to be highly expressed in gastric cancer when score 2 expression was seen (Fig. 1d), and the others as low expression (Fig. 1c).

BUBR1 score 2 expression was observed in 91 (50.3%) of the 181 patients.

Table 3 shows the relationship between the clinicopathological features and expression level of BUBR1 in patients with gastric cancer. The tumors with BUBR1 score 2 expression showed deeper invasion than those with a lower BUBR1 expression level ($P < 0.01$). Furthermore, the BUBR1 highly expressing tumors had more lymph node and liver metastases ($P < 0.01$ and $P < 0.05$, respectively). No difference was seen between BUBR1 score 0 expression and score 1 expression in gastric cancer.

DNA aneuploidy and BUBR1 expression had a significant relationship in gastric cancer. The relationship between the DNA ploidy pattern and BUBR1 expression level in gastric cancers was analyzed. The result is shown in the lower part of

Table 1. DNA ploidy and clinicopathological factors in gastric cancer

Factors	DNA ploidy		*P*-values
	Diploidy ($n = 46$)	DNA aneuploidy ($n = 70$)	
Age (mean ± SD)	61.9 ± 13.9	65.8 ± 11.3	0.116
Gender			
Male	30 (65.2)	49 (70.0)	0.589
Female	16 (34.8)	21 (30.0)	
Differentiation			
Differentiated	14 (30.4)	41 (59.4)	0.002*
Undifferentiated	32 (69.6)	28 (40.6)	
Depth of invasion			
M, SM	7 (15.2)	8 (11.4)	0.554
MP, SS, SE, SI	39 (84.8)	62 (88.6)	
Vascular involvement			
Negative	34 (73.9)	37 (53.6)	0.026**
Positive	12 (26.1)	32 (46.4)	
Lymph node metastasis			
Negative	15 (32.6)	14 (20.0)	0.127
Positive	31 (67.4)	56 (80.0)	
Liver metastasis			
Negative	45 (97.8)	67 (95.7)	0.53
Positive	1 (2.2)	3 (4.3)	
Stage			
I	13 (28.3)	12 (17.1)	0.351
II	7 (15.2)	13 (18.6)	
III	7 (15.2)	18 (25.7)	
IV	19 (41.3)	27 (38.6)	

The values in parentheses are expressed in %. *$P < 0.01$, **$P < 0.05$.
M, mucosa; MP, muscularis propria; SE, penetration of serosa; SI, invasion of adjacent structures; SM, submucosa; SS, subserosa.

Table 2. DNA ploidy and genetic factors in gastric cancer

Factors	DNA ploidy		*P*-values
	Diploidy	Aneuploidy	
TP53 status			
Wild	27 (90.0)	37 (68.5)	0.019*
Mutation	3 (10.0)	17 (31.5)	
MSI status			
MSI (–)	38 (82.6)	66 (94.3)	0.045*
MSI (+)	8 (17.4)	4 (5.7)	

The values in parentheses are expressed in %. *$P < 0.05$.
MSI, microsatellite instability.

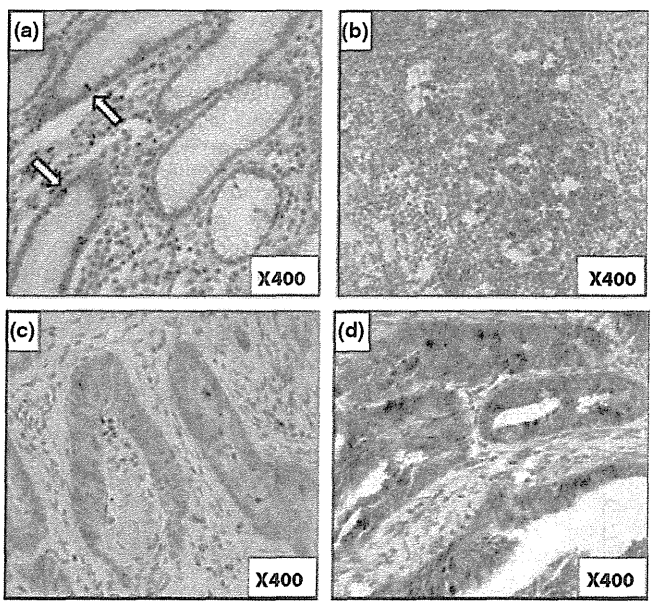

Fig. 1. Immunohistochemical staining of BUBR1 in gastric cancer. (a) BUBR1 staining in normal epithelium. Arrows show the mitotic cells whose BUBR1 staining is scored 1 (magnification, ×400). (b) BUBR1 staining in lymph follicle. BUBR1 score 1 expression was based on this intensity of BUBR1 staining (magnification, ×400). (c) BUBR1 staining in gastric cancer cells. This shows the BUBR1 score 1 expression (magnification, ×400). (d) BUBR1 staining in gastric cancer cells. This shows the BUBR1 score 2 expression, which indicates high expression of BUBR1 (magnification, ×400).

Table 3. BUBR1 expression and clinicopathological factors in gastric cancer

Factors	BUBR1 expression level		*P*-values
	Score 0,1 (n = 90)	Score 2 (n = 91)	
Age (mean ± SD)	62.5 ± 13.1	65.8 ± 10.5	0.053
Gender			
Male	60 (66.7)	61 (67.0)	0.958
Female	30 (33.3)	30 (33.0)	
Differentiation			
Differentiated	35 (38.9)	44 (48.9)	0.176
Undifferentiated	55 (61.1)	46 (51.1)	
Depth of invasion			
M, SM	17 (18.9)	5 (5.5)	0.004*
MP, SS, SE, SI	73 (81.1)	86 (94.5)	
Vascular involvement			
Negative	53 (58.9)	49 (54.4)	0.547
Positive	37 (41.1)	41 (45.6)	
Lymph node metastasis			
Negative	38 (42.2)	20 (22.0)	0.002*
Positive	52 (57.8)	71 (78.0)	
Liver metastasis			
Negative	89 (98.9)	85 (93.4)	0.044**
Positive	1 (1.1)	6 (6.6)	
Stage			
I	27 (30.0)	16 (17.6)	0.246
II	18 (20.0)	20 (22.0)	
III	20 (22.2)	22 (24.2)	
IV	25 (27.8)	33 (36.3)	
DNA ploidy			
Diploidy	28 (60.9)	18 (39.1)	0.012**
Aneuploidy	26 (39.1)	44 (62.9)	

The values in parentheses are expressed in %. *P < 0.01, **P < 0.05. M, mucosa; MP, muscularis propria; SE, penetration of serosa; SI, invasion of adjacent structures; SM, submucosa; SS, subserosa.

Table 3. Tumors with BUBR1 score 2 expression showed a significant correlation with DNA aneuploidy (P < 0.05). Not only *TP53* gene mutation but also high BUBR1 expression seemed to be an important factor for DNA aneuploidy in gastric cancer.

High expression of BUBR1 correlated with poor survival. Figure 2 shows the survival curve for patients according to expression levels of BUBR1. Patients with BUBR1 score 2 expression tumors had a significantly lower survival rate compared to patients with score 0 or 1 tumors (P < 0.05). A multivariate Cox regression analysis showed that the BUBR1 expression level was not an independent prognostic factor. This may be because in tumors with BUBR1 score 2 expression, there was a significant relationship between tumor depth and lymph node metastasis, which were strong independent prognostic factors (data not shown).

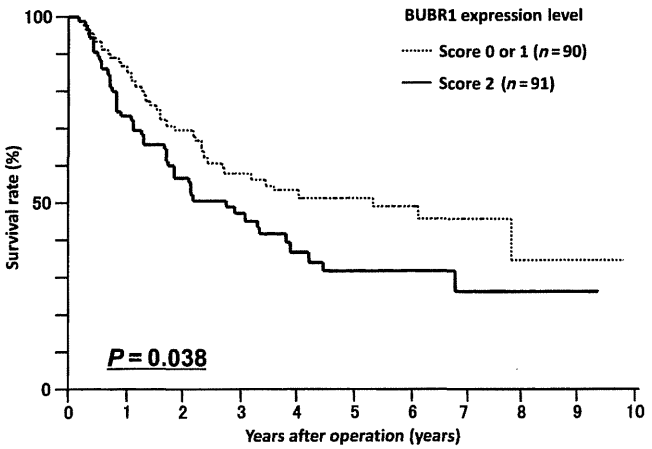

Fig. 2. Survival curve for patients with gastric cancer in relation to BUBR1 expression. Patients with BUBR1 score 2 tumors (n = 91) had a poorer survival rate compared to those with BUBR1 score 0 or 1 tumors (n = 90, P = 0.038).

High expression of BUBR1 correlated with DNA aneuploidy in gastric cancer cell lines. Next we examined the relationship between DNA ploidy and BUBR1 expression in gastric cancer cell lines. First, the DNA ploidy patterns of gastric cancer cell lines were analyzed. Growing cells on four-well chamber slide glass made it easier to compare the DNA index of gastric cancer cell lines with that of MRC-5 which was used as a normal control. LSC demonstrated that the gastric cancer cell lines MKN-28, MKN-74, NUGC-4, KATO III, and SNU-16 were aneuploid cell lines. SNU-1 and NCI-N87 (and also MRC-5) were diploid cell lines. The DNA ploidy patterns of KATO III, SNU-16, SNU-1, and NCI-N87 were the same as those shown in the ATCC cell bank information (http://www.atcc.org/).

The expression levels of BUBR1 in these cell lines were examined by real-time quantitative RT-PCR (Fig. 3a). High expression of BUBR1 was seen in MKN-28, MKN-74, and SNU-16 which were all aneuploid cell lines. A statistical analysis showed that aneuploid gastric cancer cell lines had significantly higher expression of BUBR1 compared to diploid cell lines (Fig. 3b).

Enforced expression of BUBR1 in gastric cancer cell lines led to a change in DNA ploidy pattern and high proliferation activity. Then we investigated whether or not high expression of BUBR1 would be a cause for changes to the DNA ploidy pattern.

We transfected gastric cancer cell line MKN-28 and diploid gastric cancer cell line SNU-1 with pcDNA3.1(+)-BUBR1 and an empty vector as a mock. As is shown in Figure 4a, the transfection was successful.

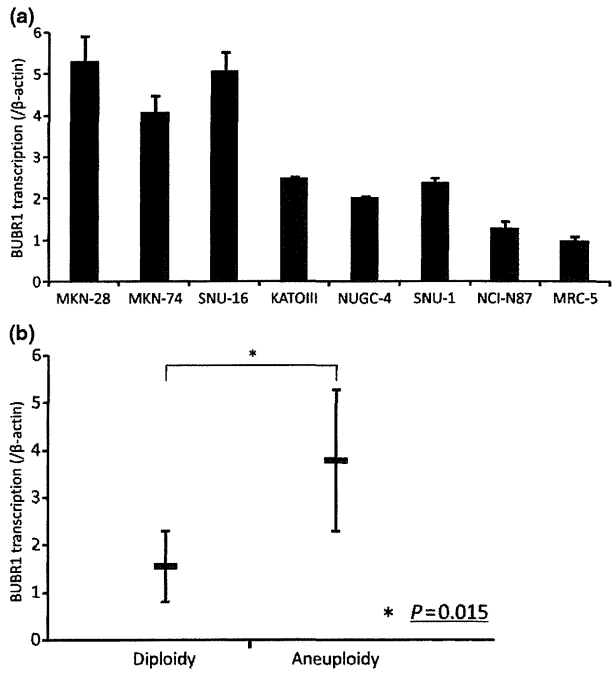

Fig. 3. DNA ploidy and BUBR1 expression in cell lines. (a) BUBR1 expression in cell lines. BUBR1 expression was determined by real-time RT-PCR. The bar indicates the SD. (b) Statistical analysis in BUBR1 expression and DNA ploidy in cell lines. DNA aneuploidy cell lines had significantly higher BUBR1 expression levels (P = 0.015).

doi: 10.1111/j.1349-7006.2009.01457.x

The DNA ploidy patterns of these cells were analyzed with LSC. The DNA indexes of the mock cells were referred as 1.0. As seen in Figure 4b, the DNA indexes of MKN-28 BUBR1 and SNU-1 BUBR1 were increased significantly compared to the mock cells. This result meant that the DNA ploidy pattern had changed in MKN-28 BUBR1 and SNU-1 BUBR1.

We also counted the cell numbers of MKN-28 BUBR1 and MKN-28 Mock to investigate the growth activity. As is shown in Figure 5a, MKN-28 BUBR1 had higher growth activity compared to MKN-28 Mock. Also, in MKN-28 BUBR1 and SNU-1 BUBR1 the expression of Ki-67 was higher than in the mock cells (Fig. 5b).

Discussion

In the current study, genomic instability was associated with DNA aneuploidy; and the chromosomal instability pathway seemed to be important in gastric carcinogenesis. Chromosomal instability and microsatellite instability pathways are reported to be exclusive in colorectal cancers.[2] However, in gastric cancer, both DNA aneuploidy and MSI (+) were observed in four (3.4%) tumors and both DNA diploidy and MSI (–) were observed in 38 (32.8%) tumors in this study. It seems that chromosomal instability and microsatellite instability pathways are not always mutually exclusive in gastric cancer, and additional mechanisms, such as the CpG island methylator phenotype (CIMP), may contribute to gastric carcinogenesis.[35]

It is well known that mutation in the *TP53* gene contributes to DNA aneuploidy. In our study, DNA aneuploidy and *TP53* gene mutation were significantly correlated. However, the frequency of the *TP53* gene mutation (23.8%) was less than DNA aneuploidy (60.3%). Thus it seemed that the mutation in the *TP53* gene did not explain all the DNA aneuploidy in gastric cancers.[3]

This study revealed that, by immunohistochemical staining, high expression of BUBR1, a key molecule in the spindle assembly checkpoint, had a significant correlation with DNA

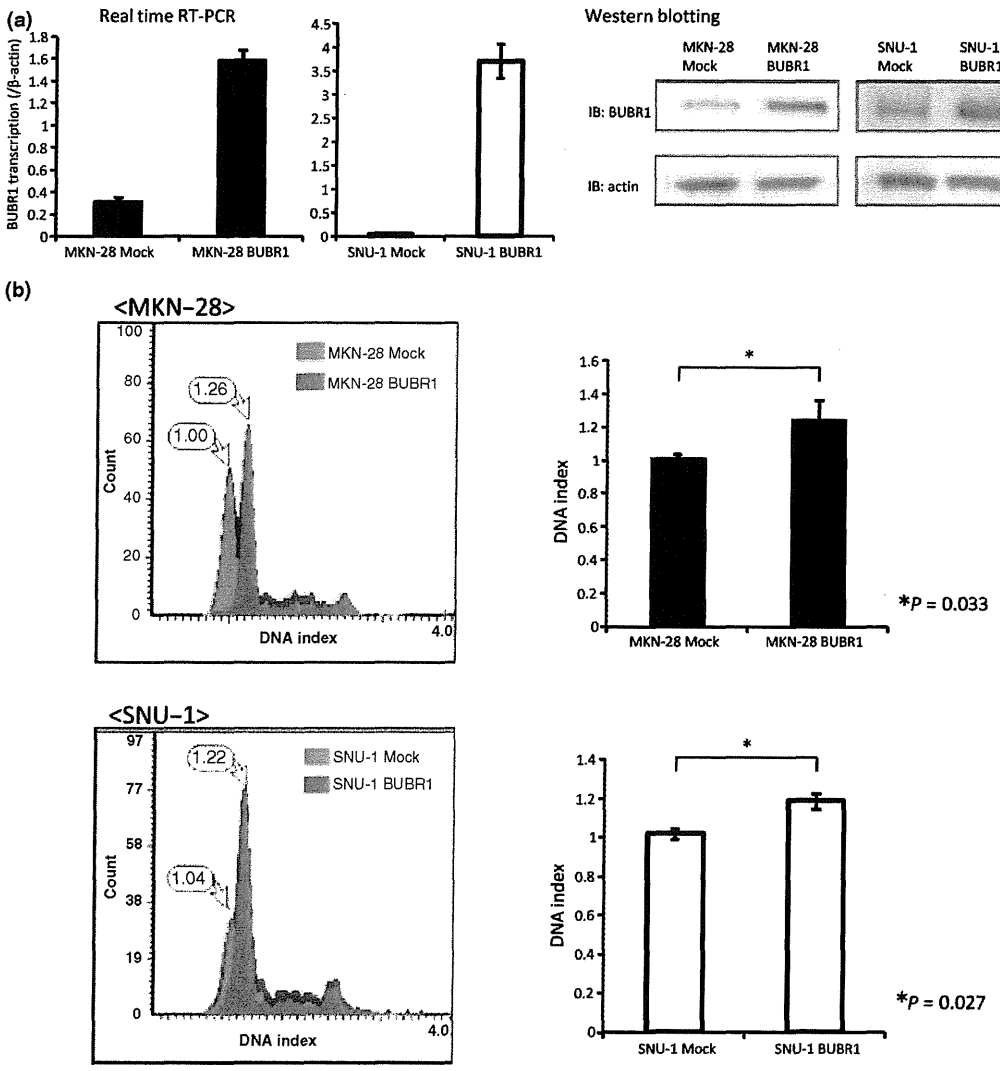

Fig. 4. Enforced expression of BUBR1 in gastric cancer cell lines led to a change in DNA ploidy pattern. (a) Establishing BUBR1 highly expressed gastric cancer cell line MKN-28 and SNU-1. The expression levels of BUBR1 in the mock cells and BUBR1-enforced cells were investigated by real-time RT-PCR and Western blotting. High expression of BUBR1 can be seen in BUBR1-enforced cells at both the mRNA and protein level. (b) DNA ploidy pattern change in BUBR1 highly expressed cells. The DNA ploidy patterns were investigated by laser scanning cytometry. The DNA indexes of the mock cells were determined as 1.0. The change in DNA ploidy pattern can be seen in MKN-28 BUBR1 and SNU-1 BUBR1. Also the DNA index was significantly changed in MKN-28 BUBR1 and SNU-1 BUBR1 compared to the mock cells (right panel, $P = 0.033$ and $P = 0.027$, respectively).

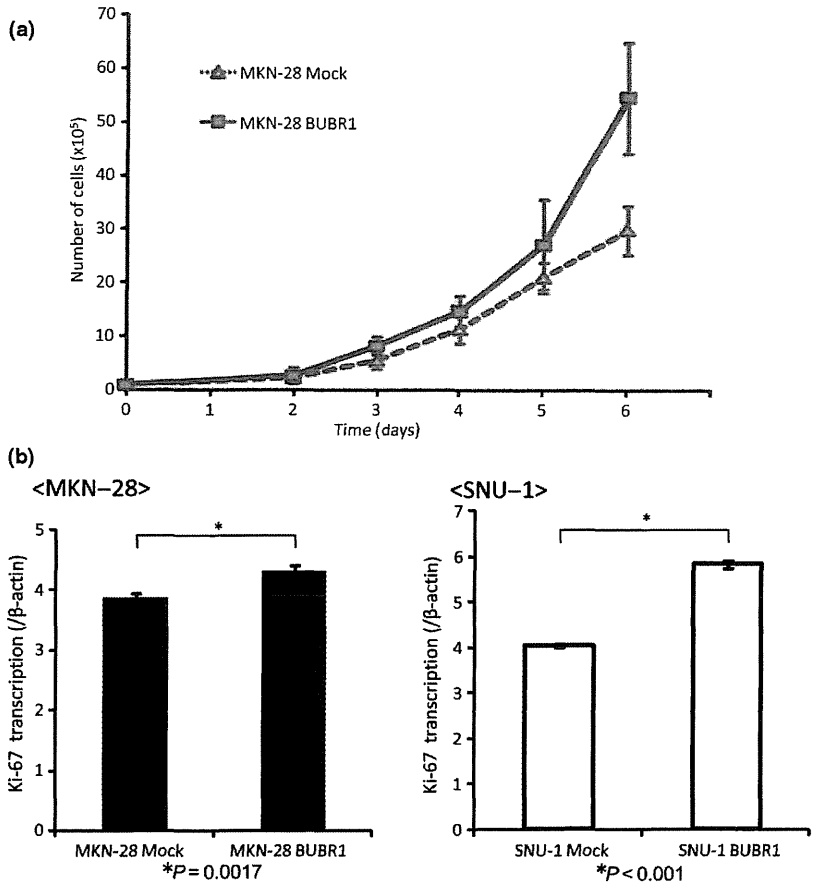

Fig. 5. High expression of BUBR1 had high proliferation activity in gastric cancer cell lines. (a) The growth curve of MKN-28 Mock and MKN-28 BUBR1. MKN-28 BUBR1 had higher growth activity. (b) Ki-67 expression in mock cells and BUBR1 highly expressed cells. Ki-67 expression was determined by real-time RT-PCR. Higher expression of Ki-67 was seen in BUBR1 highly expressed cells.

aneuploidy in gastric cancer. This result was consistent with the study on bladder cancer by Yamamoto *et al.*[19] Also the gastric cancer cell lines which showed DNA aneuploidy had higher BUBR1 expression in comparison to DNA diploid cell lines. High expression of BUBR1 may be an important factor for DNA aneuploidy and may contribute to chromosomal instability.

In this study, we also found that the enforced expression of BUBR1 in the gastric cancer cell line MKN-28 and the diploid gastric cancer cell line SNU-1 contributed to the change to the DNA ploidy pattern compared with mock cells. The mechanism for changes to the DNA ploidy pattern in the BUBR1 highly expressed cell line is unclear. It is known that BUBR1 forms a complex with Bub3, Mad2, and Cdc20 at the spindle assembly checkpoint and thus inhibits Cdc20 activity.[36] In gastric cancer cells with high BUBR1 expression, the formation of this complex might be compromised and the spindle assembly checkpoint may be overridden, which may result in DNA aneuploidy.

When BUBR1 is depleted in human cells, it results in chromosome misalignment,[37] and its suppression is invariably lethal due to massive chromosomal loss.[38] It is reported that reduction in BUBR1 levels in $Apc^{Min/+}$ mice, which carry one mutant *Apc* allele encoding a truncated protein that causes intestinal neoplasias, resulted in a 10-fold increase in the number of tumors that developed by the same age, and these tumors were also of a higher grade.[39] Moreover, the overexpression of Mad2, another molecule at the spindle assembly checkpoint, caused DNA aneuploidy and carcinogenesis in mice.[40] An abnormal expression level in spindle assembly checkpoint molecules, including BUBR1, seems to be important for carcinogenesis.

On the other hand, we also found that high expression of BUBR1 correlated with malignant features and liver metastasis in gastric cancer. And those tumors demonstrating high BUBR1 expression were associated with a poorer survival rate compared to the tumors with low expression of BUBR1. These results might reflect the fact that BUBR1 high-expressed tumors have a high proliferation activity. In fact, the current study showed that with enforced expression of BUBR1 in MKN-28 gastric cancer cell line, the growth of the cells increased. And in both MKN-28 BUBR1 and SNU-1 BUBR1, the expression of Ki-67 increased significantly. It has been reported that enforced expression of BUBR1 in HeLa cells increased the mitotic index.[10] Also, Grabsh *et al.*[41] reported that BUBR1 high expression had a significant relationship with Ki-67 expression in gastric cancer clinical samples, which was a similar result to our study in gastric cancer cell lines.

Taken together, the high expression of BUBR1 may result in the proliferation of tumor cells and DNA aneuploidy.

A high expression of BUBR1 may correlate with DNA aneuploidy in gastric cancer. However, a question remains. As malignancies which show DNA aneuploidy have aberrant chromosome numbers, high expression of BUBR1 may be an effect of the DNA aneuploidy. In our study, we only observed the DNA ploidy pattern change in MKN-28 and SNU-1 gastric cancer cells. Further studies on BUBR1 and other factors in the spindle assembly checkpoint as a cause or effect of chromosomal instability are necessary.

Association between BUBR1 expression and taxane sensitivity was reported in breast and esophageal cancer.[42,43] Our succinic dehydrogenase inhibition (SDI) test data of gastric cancer specimens, however, did not indicate significant association between BUBR1 expression and taxane sensitivity (data not shown). Therefore, we may not be able to predict the therapeutic

doi: 10.1111/j.1349-7006.2009.01457.x

effect of taxane from the expression level of BUBR1 in gastric cancer. Recently, tumor necrosis factor-related apoptosis-inducing ligand (TRAIL) has attracted interest as an anticancer treatment when used in conjunction with standard chemotherapy, such as the taxanes. Kim *et al.* reported that adding TRAIL to the taxanes accentuates the degradation of BUBR1 and induces cancer cell death.[44] Using TRAIL with the taxanes in BUBR1 high-expressed gastric cancers might therefore be a successful treatment.

In conclusion, the high expression of BUBR1 was associated with DNA aneuploidy and was also correlated with tumor invasion and metastasis in gastric cancer. The elucidation of the spindle assembly checkpoint may therefore help to clarify the mechanism for DNA aneuploidy and progression in gastric cancer.

Acknowledgments

We thank Ms Y. Kubota for her wonderful work in preparing the immunohistochemistry samples. Also we thank Ms T. Shishino, Ms K. Yamashita, and Ms K. Tagata for their technical assistance.

References

1 Bignold LP, Coghlan B, Jersmann H. David Paul Hansemann: chromosomes and the origin of the cancerous features of tumor cells. *Cell Oncol* 2009; **31**: 61.
2 Lengauer C, Kinzler KW, Vogelstein B. Genetic instability in colorectal cancers. *Nature* 1997; **386**: 623–7.
3 Duensing A, Duensing S. Guilt by association? p53 and the development of aneuploidy in cancer. *Biochem Biophys Res Commun* 2005; **331**: 694–700.
4 Smith ML, Fornace AJ Jr. Genomic instability and the role of p53 mutations in cancer cells. *Curr Opin Oncol* 1995; **7**: 69–75.
5 Hartwell LH, Weinert TA. Checkpoints: controls that ensure the order of cell cycle events. *Science (New York, NY)* 1989; **246**: 629–34.
6 Amon A. The spindle checkpoint. *Curr Opin Genet Dev* 1999; **9**: 69–75.
7 van Deursen JM. Rb loss causes cancer by driving mitosis mad. *Cancer Cell* 2007; **11**: 1–3.
8 Jablonski SA, Chan GK, Cooke CA, Earnshaw WC, Yen TJ. The hBUB1 and hBUBR1 kinases sequentially assemble onto kinetochores during prophase with hBUBR1 concentrating at the kinetochore plates in mitosis. *Chromosoma* 1998; **107**: 386–96.
9 Fang G. Checkpoint protein BubR1 acts synergistically with Mad2 to inhibit anaphase-promoting complex. *Mol Biol Cell* 2002; **13**: 755–66.
10 Wu H, Lan Z, Li W *et al.* p55CDC/hCDC20 is associated with BUBR1 and may be a downstream target of the spindle checkpoint kinase. *Oncogene* 2000; **19**: 4557–62.
11 Ge S, Skaar JR, Pagano M. APC/C- and Mad2-mediated degradation of Cdc20 during spindle checkpoint activation. *Cell Cycle* 2009; **8**: 167–71.
12 Kim HS, Jeon YK, Ha GH *et al.* Functional interaction between BubR1 and securin in an anaphase-promoting complex/cyclosomeCdc20-independent manner. *Cancer Res* 2009; **69**: 27–36.
13 Matsuura S, Ito E, Tauchi H, Komatsu K, Ikeuchi T, Kajii T. Chromosomal instability syndrome of total premature chromatid separation with mosaic variegated aneuploidy is defective in mitotic-spindle checkpoint. *Am J Hum Genet* 2000; **67**: 483–6.
14 Matsuura S, Matsumoto Y, Morishima K *et al.* Monoallelic BUB1B mutations and defective mitotic-spindle checkpoint in seven families with premature chromatid separation (PCS) syndrome. *Am J Med Genet* 2006; **140**: 358–67.
15 Myrie KA, Percy MJ, Azim JN, Neeley CK, Petty EM. Mutation and expression analysis of human BUB1 and BUB1B in aneuploid breast cancer cell lines. *Cancer Lett* 2000; **152**: 193–9.
16 Sato M, Sekido Y, Horio Y *et al.* Infrequent mutation of the hBUB1 and hBUBR1 genes in human lung cancer. *Jpn J Cancer Res* 2000; **91**: 504–9.
17 Pinto M, Vieira J, Ribeiro FR *et al.* Overexpression of the mitotic checkpoint genes BUB1 and BUBR1 is associated with genomic complexity in clear cell kidney carcinomas. *Cell Oncol* 2008; **30**: 389–95.
18 Scintu M, Vitale R, Prencipe M *et al.* Genomic instability and increased expression of BUB1B and MAD2L1 genes in ductal breast carcinoma. *Cancer Lett* 2007; **254**: 298–307.
19 Yamamoto Y, Matsuyama H, Chochi Y *et al.* Overexpression of BUBR1 is associated with chromosomal instability in bladder cancer. *Cancer Genet Cytogenet* 2007; **174**: 42–7.
20 Japanese Gastric Cancer A. Japanese classification of gastric carcinoma – 2nd english edition. *Gastric Cancer* 1998; **1**: 10–24.
21 Burum-Auensen E, De Angelis PM, Schjolberg AR, Kravik KL, Aure M, Clausen OPF. Subcellular localization of the spindle proteins Aurora A, Mad2, and BUBR1 assessed by immunohistochemistry. *J Histochem Cytochem* 2007; **55**: 477–86.
22 Burum-Auensen E, DeAngelis PM, Schjolberg AR, Roislien J, Andersen SN, Clausen OPF. Spindle proteins Aurora A and BUB1B, but not Mad2, are aberrantly expressed in dysplastic mucosa of patients with longstanding ulcerative colitis. *J Clin Pathol* 2007; **60**: 1403–8.
23 Kamada T, Sasaki K, Tsuji T, Todoroki T, Takahashi M, Kurose A. Sample preparation from paraffin-embedded tissue specimens for laser scanning cytometric DNA analysis. *Cytometry* 1997; **27**: 290–4.
24 Sasaki K, Kurose A, Miura Y, Sato T, Ikeda E. DNA ploidy analysis by laser scanning cytometry (LSC) in colorectal cancers and comparison with flow cytometry. *Cytometry* 1996; **23**: 106–9.
25 Furuya T, Uchiyama T, Murakami T *et al.* Relationship between chromosomal instability and intratumoral regional DNA ploidy heterogeneity in primary gastric cancers. *Clin Cancer Res* 2000; **6**: 2815–20.
26 Hiddemann W, Schumann J, Andreef M *et al.* Convention on nomenclature for DNA cytometry. Committee on Nomenclature, Society for Analytical Cytology. *Cancer Genet Cytogenet* 1984; **13**: 181–3.
27 Oda S, Oki E, Maehara Y, Sugimachi K. Precise assessment of microsatellite instability using high resolution fluorescent microsatellite analysis. *Nucleic Acids Res* 1997; **25**: 3415–20.
28 Boland CR, Thibodeau SN, Hamilton SR *et al.* A National Cancer Institute Workshop on Microsatellite Instability for cancer detection and familial predisposition: development of international criteria for the determination of microsatellite instability in colorectal cancer. *Cancer Res* 1998; **58**: 5248–57.
29 Kues WA, Anger M, Carnwath JW, Paul D, Motlik J, Niemann H. Cell cycle synchronization of porcine fetal fibroblasts: effects of serum deprivation and reversible cell cycle inhibitors. *Biol Reprod* 2000; **62**: 412–9.
30 Shichiri M, Yoshinaga K, Hisatomi H, Sugihara K, Hirata Y. Genetic and epigenetic inactivation of mitotic checkpoint genes hBUB1 and hBUBR1 and their relationship to survival. *Cancer Res* 2002; **62**: 13–7.
31 Joyce NC, Navon SE, Roy S, Zieske JD. Expression of cell cycle-associated proteins in human and rabbit corneal endothelium in situ. *Invest Ophthalmol Vis Sci* 1996; **37**: 1566–75.
32 Baba H, Korenaga D, Kakeji Y, Haraguchi M, Okamura T, Maehara Y. DNA ploidy and its clinical implications in gastric cancer. *Surgery* 2002; **131**: S63–70.
33 Setala LP, Nordling S, Kosma VM *et al.* Comparison of DNA ploidy and S-phase fraction with prognostic factors in gastric cancer. *Anal Quant Cytol Histol* 1997; **19**: 524–32.
34 Chi YH, Jeang KT. Aneuploidy and cancer. *J Cell Biochem* 2007; **102**: 531–8.
35 Ottini L, Falchetti M, Lupi R *et al.* Patterns of genomic instability in gastric cancer: clinical implications and perspectives. *Ann Oncol* 2006; **17** (Suppl 7): vii97–102.
36 Davenport J, Harris LD, Goorha R. Spindle checkpoint function requires Mad2-dependent Cdc20 binding to the Mad3 homology domain of BubR1. *Exp Cell Res* 2006; **312**: 1831–42.
37 Lampson MA, Kapoor TM. The human mitotic checkpoint protein BubR1 regulates chromosome-spindle attachments. *Nat Cell Biol* 2005; **7**: 93–8.
38 Kops GJ, Foltz DR, Cleveland DW. Lethality to human cancer cells through massive chromosome loss by inhibition of the mitotic checkpoint. *Proc Natl Acad Sci U S A* 2004; **101**: 8699–704.
39 Rao CV, Yang YM, Swamy MV *et al.* Colonic tumorigenesis in BubR1 +/-ApcMin/+ compound mutant mice is linked to premature separation of sister chromatids and enhanced genomic instability. *Proc Natl Acad Sci U S A* 2005; **102**: 4365–70.
40 Sotillo R, Hernando E, Diaz-Rodriguez E *et al.* Mad2 overexpression promotes aneuploidy and tumorigenesis in mice. *Cancer Cell* 2007; **11**: 9–23.
41 Grabsch H, Takeno S, Parsons WJ *et al.* Overexpression of the mitotic checkpoint genes BUB1, BUBR1, and BUB3 in gastric cancer – association with tumour cell proliferation. *J Pathol* 2003; **200**: 16–22.
42 McGrogan BT, Gilmartin B, Carney DN, McCann A. Taxanes, microtubules and chemoresistant breast cancer. *Biochim Biophys Acta* 2008; **1785**: 96–132.
43 Tanaka K, Mohri Y, Ohi M *et al.* Mitotic checkpoint genes, hsMAD2 and BubR1, in oesophageal squamous cancer cells and their association with 5-fluorouracil and cisplatin-based radiochemotherapy. *Clin Oncol (R Coll Radiol)* 2008; **20**: 639–46.
44 Kim M, Liao J, Dowling ML *et al.* TRAIL inactivates the mitotic checkpoint and potentiates death induced by microtubule-targeting agents in human cancer cells. *Cancer Res* 2008; **68**: 3440–9.

Surg Today (2010) 40:626–631
DOI 10.1007/s00595-009-4135-1

SURGERY TODAY

Original Article

Impact of Perioperative Peripheral Blood Values on Postoperative Complications After Esophageal Surgery

HIROSHI SAEKI[1], TAKANOBU MASUDA[1], SATOKO OKADA[1], KOJI ANDO[1], MASAHIKO SUGIYAMA[1], KEIJI YOSHINAGA[1], KAZUYA ENDO[1], NORIAKI SADANAGA[1], YASUNORI EMI[1,2], YOSHIHIRO KAKEJI[1], MASARU MORITA[1], NATSUMI YAMASHITA[2], and YOSHIHIKO MAEHARA[1]

Departments of [1]Surgery and Science and [2]Innovative Applied Oncology, Graduate School of Medical Sciences, Kyushu University, 3-1-1 Maidashi, Higashi-ku, Fukuoka 812-8582, Japan

Abstract

Purpose. Prediction of the postoperative course of esophagectomy is an important part of the strict perioperative management of patients undergoing surgery for esophageal cancer.

Methods. To evaluate their clinical importance, peripheral blood values, including white blood cell count (WBC), lymphocyte count, and the levels of total protein, transferrin, factor XIII, D-dimer, fibrin, and fibrinogen degradation products (FDP) were measured before and after esophagectomy for esophageal cancer in 24 patients.

Results. The preoperative WBC and the pre- and postoperative lymphocyte count were decreased remarkably in patients who received preoperative chemoradiotherapy. The values of perioperative serum transferrin were significantly lower in patients with postoperative pneumonia than in those without. The activity of plasma factor XIII was suppressed on postoperative day (POD) 7 in patients with pneumonia and on POD 14 in patients with leakage.

Conclusions. These results suggest that patients who receive preoperative chemoradiotherapy are potentially immunosuppressed, the preoperative serum transferrin level is a possible predictive marker of postoperative pneumonia, and suppression of factor XIII activity is related to anastomotic insufficiency.

Key words Esophagectomy · Preoperative therapy · Pneumonia · Leakage · Transferrin · Factor XIII

Reprint requests to: H. Saeki
Received: December 12, 2008 / Accepted: April 27, 2009

Introduction

Surgery remains the standard therapy for esophageal cancer because it provides the best chance of cure.[1] However, resection and reconstruction of the esophagus is one of the most invasive treatments for cancers of the digestive organs. Although the surgical techniques and perioperative management of esophageal surgery have improved remarkably, the morbidity and mortality rates are still high in comparison with those associated with other procedures.[2–5] Esophageal cancer usually occurs in older patients who often have coexisting diseases, particularly of the heart and lungs, and these comorbidities can impair the tolerance of patients to the invasiveness of an esophagectomy. Analyses of the preoperative risk factors of complications have been carried out;[6] however, clinically practical methods of assessing operative risks are still required. The present study prospectively evaluates the perioperative peripheral blood values of measures of immunity, nutrition, and wound healing, to predict the postoperative clinical course, focusing on preoperative treatment and postoperative pneumonia and leakage. Our data clarified the relationship between the various values and the postoperative clinical course and the likelihood of postoperative complications after esophagectomy.

Patients and Methods

Patients

The subjects of this study were 24 patients who underwent esophageal resection and reconstruction for thoracic esophageal cancer in the Department of Surgery and Science, Graduate School of Medical Sciences, Kyushu University, between 2007 and 2008. The median age was 62 years (range, 47–78 years) and there were 21 men and 3 women. All cases were in a World Health

Organization (WHO) performance status of either 0 or 1. Squamous cell carcinoma was diagnosed histologically in all the patients. Eight of the patients received preoperative chemoradiotherapy, three of whom received definitive chemoradiotherapy with more than 50 Gy of radiation.

Treatment Procedures

Thoracic esophageal cancer was treated with either subtotal esophagectomy with an anterolateral right thoracotomy and cervical anastomosis, or distal esophagectomy with an anterolateral right thoracotomy, laparotomy, and intrathoracic anastomosis. Patients with carcinoma of the upper- or mid-thoracic esophagus or advanced carcinoma of the lower thoracic esophagus, who were in good health otherwise, generally underwent subtotal esophagectomy via a cervico-right thoracoabdominal approach. To adjust the background of the surgical procedures, only patients who underwent subtotal esophagectomy with an anterolateral right thoracotomy and cervical anastomosis were included in this study. Reconstruction was accomplished using a pulled-up gastric tube in all patients. Three-field and two-field lymph node dissections were performed in 18 (75.0%) and 6 (25.0%) patients, respectively. Five patients with locally advanced cancer received preoperative chemoradiotherapy, consisting of 35–42 Gy of radiation and cisplatin plus 5-fluorouracil. Three patients received definitive chemoradiotherapy, consisting of more than 50 Gy of radiation and cisplatin plus 5-fluorouracil.

Measurement of Peripheral Blood Values

The blood was analyzed within 1 week before surgery, and then on postoperative day (POD) 7 and 14. We measured the white blood cell count (WBC), the lymphocyte count, and the levels of total protein, transferrin, factor XIII, D-dimer, fibrin, and fibrinogen degradation products (FDP). The normal ranges of each measurement are as follows: WBC, 3500–9000/μl; lymphocytes, 1800–5300/μl; total protein, 6.7–8.3 g/dl; transferrin, 190–300 mg/dl; factor XIII, 55%–145%; D-dimer, ≥1 μg/dl; FDP, > 5 μg/dl.

Statistical Analysis

The clinicopathological factors and the various peripheral blood values were compared in relation to the preoperative treatment, postoperative pneumonia (defined as an infiltration shadow on chest X-rays and a positive bacterial culture of sputum), and cervical anastomotic leakage (confirmed by postoperative esophagogram or saliva discharge through the fistula). Significant differences were established using Fisher's exact test in the distribution frequencies of the data in Tables 1–3 except for age. The Mann–Whitney *U*-test was applied for differences in age, the operative time, blood loss, and the values of these parameters between the groups. A P

Table 1. Clinicopathological features according to preoperative treatment

Factor	Preoperative treatment	
	No (n = 16)	Yes (n = 8)
Sex		
Male	14 (87.5)	7 (87.5)
Female	2 (12.5)	1 (12.5)
Age (mean ± SD)	62.2 ± 6.8	61.5 ± 10.1
pStage		
0, I, II	10 (62.5)	5 (62.5)
III, IV	6 (37.5)	3 (37.5)
Postoperative pneumonia		
(–)	12 (75.0)	6 (75.0)
(+)	4 (25.0)	2 (25.0)
Postoperative leakage		
(–)	12 (75.0)	6 (75.0)
(+)	4 (25.0)	2 (25.0)

No significant difference was observed between the two groups. The numbers in parentheses are percentages

Table 2. Clinicopathological features and the clinical development of postoperative pneumonia

Factor	Postoperative pneumonia	
	No (n = 18)	Yes (n = 6)
Sex		
Male	15 (83.3)	6 (100.0)
Female	3 (16.7)	0 (0)
Age (mean ± SD)*	60.0 ± 7.7	67.8 ± 4.9
pStage		
0, I, II	12 (66.7)	3 (50.0)
III, IV	6 (33.3)	3 (50.0)
Postoperative leakage		
(–)	15 (83.3)	3 (50.0)
(+)	3 (16.7)	3 (50.0)

*The ages of the patients in the two groups differed significantly (P < 0.05). The numbers in parentheses are percentages

Table 3. Clinicopathological features and the clinical development of postoperative leakage

Factor	Postoperative leakage	
	No (n = 18)	Yes (n = 6)
Sex		
Male	15 (83.3)	6 (100.0)
Female	3 (16.7)	0 (0)
Age (mean ± SD)	61.8 ± 7.9	62.5 ± 8.8
pStage		
0, I, II	10 (55.6)	5 (83.3)
III, IV	8 (44.4)	1 (16.7)

No significant difference was observed between the two groups. The numbers in parentheses are percentages

value of less than 0.05 was considered significant. Data were analyzed using the StatView software package (Abacus Concepts, Berkeley, CA, USA).

Results

Patient Characteristics According to Preoperative Treatment and the Postoperative Complications of Pneumonia and Anastomotic Leakage

There were no significant differences between the two groups in sex, mean age, pathological stage of esophageal cancer, or in the incidences of postoperative pneumonia and anastomotic leakage (Tables 1–3). The mean age of the patients who suffered from postoperative pneumonia was significantly higher than that of those who did not (67.8 vs 60.0 years old, respectively; $P < 0.05$). There were no significant differences between the groups in any of the factors related to postoperative leakage. The extent of lymph node dissection, the operative time, and the blood loss had no association with any of the preoperative treatments, postoperative pneumonia, or anastomotic leakage.

Relationship Between Peripheral Blood Values and Preoperative Treatment

We compared the peripheral blood values between the preoperative treatment group and the no treatment group (Fig. 1). The preoperative WBC and lymphocyte count, and the lymphocyte count on PODs 7 and 14 were all significantly lower in the patients who received preoperative chemoradiation therapy (4325/μl vs 5622/μl, 759/μl vs 1745/μl, 582/μl vs 1294/μl, 548/μl vs 1367/μl, respectively; all $P < 0.05$). There were no significant differences in transferrin, factor XIII, D-dimer, and FDP.

Peripheral Blood Values in Relation to Postoperative Pneumonia

The nutrition markers were significantly lower at some points in the patients who suffered pneumonia than in those who did not (Fig. 2) (total protein on POD 7, 5.5 g/dl vs 6.1 g/dl; preoperative transferrin, 181 mg/dl vs 224 mg/dl; transferrin on POD 7, 112 mg/dl vs 177 mg/dl; transferrin on POD 14, 157 mg/dl vs 220 mg/dl; all $P < 0.05$). The activity of plasma factor XIII on POD 7 in the pneumonia group was significantly lower than that in the group without pneumonia (35.7% vs 55.9%; $P < 0.05$). There were no significant differences in WBC, lymphocyte, D-dimer, and FDP.

Peripheral Blood Values in Relation to Postoperative Leakage

There was no significant difference in plasma factor XIII activity on POD 14 between the two groups (Fig. 3) (63% in the leakage group vs 85% in the no leakage group; $P < 0.05$). There were also no significant differences in WBC, lymphocyte, total protein, transferrin, D-dimer, and FDP.

Discussion

Mortality rates after esophageal surgery range from 2% to 25%,[7] and are primarily determined by the develop-

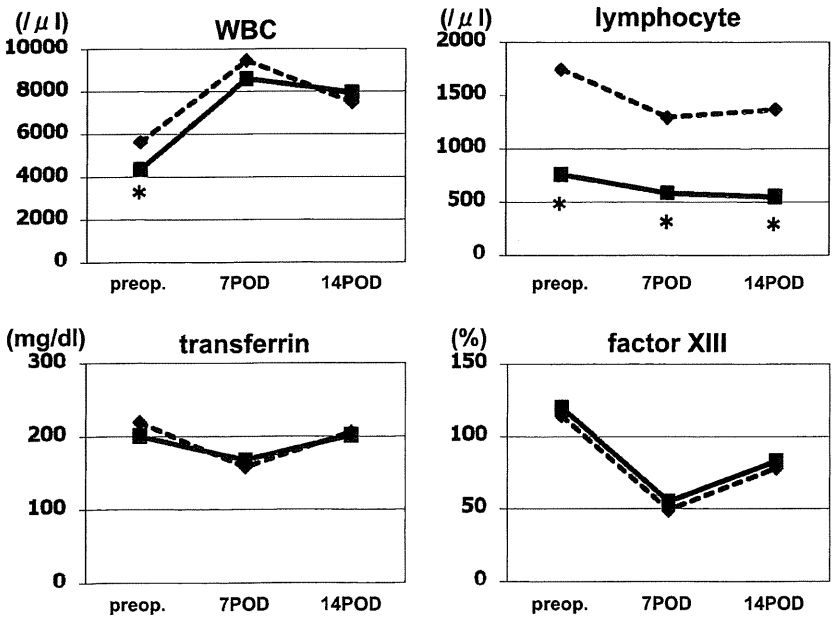

Fig. 1. Differences in peripheral blood values according to preoperative treatment. *Diamonds* (group A), patients who did not receive preoperative treatment ($n = 16$); *squares* (group B), patients who received preoperative treatment ($n = 8$). *$P < 0.05$

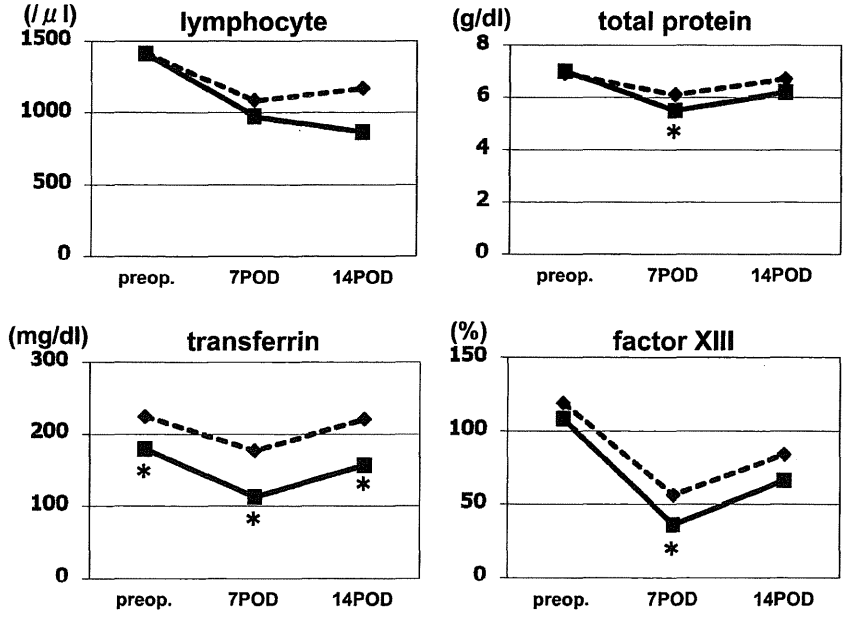

Fig. 2. Differences in peripheral blood values according to the development of postoperative pneumonia. *Diamonds* (group C), patients without postoperative pneumonia (n = 18); *squares* (group D), patients with postoperative pneumonia (n = 6). *P < 0.05

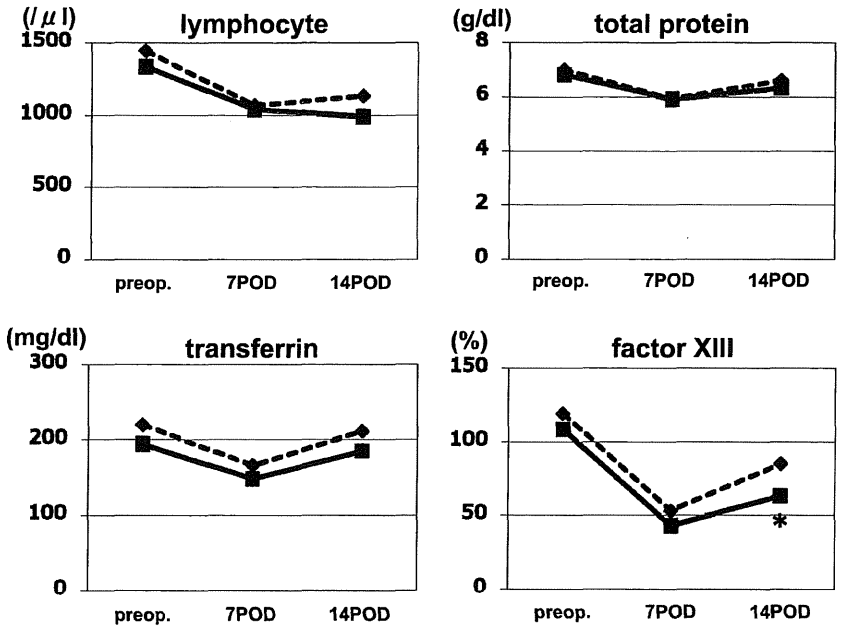

Fig. 3. Differences in peripheral blood values according to postoperative leakage. *Diamonds* (group E), patients without postoperative leakage (n = 18); *squares* (group F), patients with postoperative leakage (n = 6). *P < 0.05

ment of pulmonary complications and anastomotic leakage.[8–10] Various risk analyses have also revealed impaired heart, liver, and respiratory systems, in addition to the patients' age and general condition as independent predictors of morbidity and mortality.[7,11–13] However, no perioperative marker has been established to predict the postoperative course. We evaluated the blood cell counts as an inflammatory marker, the total protein, and transferrin as nutrition markers, and factor XIII, D-dimer, and FDP as coagulation markers. These markers are considered to be representative of the perioperative condition of patients with esophageal cancer.

The preoperative WBC and the pre- and postoperative lymphocyte counts were significantly lower in the patients who received preoperative treatment; however, the factors associated with the clinical benefit of preoperative chemoradiotherapy and its adverse effects on the development of postoperative complications are still unclear. According to some reports, preoperative chemoradiotherapy resulted in an increase of the inci-

dence of postoperative complications after esophagectomy,[14-16] whereas according to others, the incidences were similar with and without preoperative chemoradiotherapy.[17-19] An analysis of 1000 consecutive patients with esophageal cancer[3] revealed preoperative treatment as an independent factor associated with the postoperative development of pulmonary complications. Multiple immunologic values examined in patients with esophageal cancer revealed that preoperative treatment induced significant reductions in the phytohemagglutinin (PHA) response and natural killer (NK) activity.[20] Preoperative treatment did not affect the incidence of postoperative complications in the current series, probably because of the small number of patients evaluated. Nevertheless, our data indicate that patients who receive preoperative chemoradiotherapy are in a potentially immunosuppressed state and they should therefore be managed carefully.

Most operative deaths are caused by severe pulmonary complications,[3,21,22] so their prevention is of the utmost importance for decreasing the incidence of postoperative deaths. Serum transferrin is associated with overall protein synthesis. Protein synthesis is suppressed after esophageal surgery because of the host response to stress.[23] In this study, the pre- and postoperative levels of serum transferrin were significantly lower in the patients who suffered postoperative pneumonia than in those who did not. These data suggest that the preoperative level of serum transferrin could be a predictor of postoperative pneumonia. Since the serum transferrin level is a marker reflecting the nutritional status of the acute phase, this also suggests that preoperative enteral immunonutrition[23] may promote the patient's postoperative nutritional status and prevent the development of pneumonia. To evaluate the importance of the changes in transferrin values during the clinical course, the preoperative values were set as 100%, and then the values on PODs 7 and 14 were compared. Although both values tended to be lower in the pneumonia group patients than in the patients without pneumonia (data not shown), the differences were not significant. We think that depression of the absolute value of transferrin is a truer indicator of the development of postoperative pneumonia.

Esophagogastric anastomotic leakage is the most feared surgical complication of esophageal resection and reconstruction. Traditionally, symptomatic postoperative esophageal fistula is repaired surgically, and if this is unsuccessful, esophageal diversion is done, which prolongs hospitalization and delays oral hydration and nutrition. Coagulation factor XIII was first described by Laki and Lóránd in 1948 as a "fibrin-stabilizing factor."[24] Factor XIII is the last enzyme (plasma protransglutaminase) in the physiological coagulation cascade, and it is also important for the proliferation and immigration of fibroblasts in wound healing. Since factor XIII is required for normal wound healing, we investigated the temporal changes in plasma factor XIII following esophagectomy. The plasma factor XIII activity on POD 14 was significantly decreased in the patients with postoperative leakage. Notably, the activity of factor XIII on POD 7 in the patients with postoperative pneumonia was significantly lower than that in those without pneumonia. Taking into consideration that three of six patients with postoperative pneumonia suffered subsequent anastomotic insufficiency, depression of the activity of factor XIII associated with pneumonia might be related to poor wound healing of the anastomotic site. Factor XIII has been used in the treatment of ulceration caused by pressure, large burns, sepsis, and acute liver disorders.[25] Further clinical investigations on the effectiveness of factor XIII for patients with anastomotic leakage are warranted. Other factors that have been reported to be useful markers for predicting postoperative complications include serum acute phase reactants and several cytokines such as interleukin-6 and gene polymorphism.[26] However, the measurement of these factors, other than acute phase reactants, is complex and expensive. Thus, we measured the general peripheral blood values in patients with esophageal cancer, and the results are considered meaningful from the viewpoint of cost-effectiveness.

In conclusion, the perioperative peripheral blood values in patients undergoing surgery for esophageal cancer revealed decreased WBC and lymphocyte counts in patients who received preoperative treatment, lower levels of serum transferrin in patients who suffered postoperative pneumonia, and a positive association of decreased postoperative plasma factor XIII with anastomotic insufficiency. Further studies on the roles of these and other markers in a larger group of patients with esophageal cancer are required to fully understand the role of peripheral blood measurements in the perioperative management.

Acknowledgments. We thank Brian Quinn for assisting with the preparation of the manuscript. This work was supported in part by a Grant-in-Aid from the Ministry of Education, Culture, Sport, Science and Technology of Japan.

References

1. Wu PC, Posner M. The role of surgery in the management of oesophageal cancer. Lancet Oncol 2003;4:481–8.
2. Jamieson GG, Mathew G, Ludemann R, Wayman J, Myers JC, Devitt PG. Postoperative mortality following oesophagectomy and problem in reporting its rate. Br J Surg 2004;9:943–7.
3. Morita M, Yoshida R, Ikeda K Egashira A, Oki E, Sadanaga N, et al. Advances in esophageal cancer surgery in Japan: an analysis of 1000 consecutive patients treated at a single institute. Surgery 2008;143:499–508.

4. Shichinohe T, Hirano S, Kondo S. Video-assisted esophagectomy for esophageal cancer. Surg Today 2008;38:206–13.
5. Li SH, Wang Z, Liu XY, Liu FY, Sun ZY, Xue H. Lymph node micrometastasis: a predictor of early tumor relapse after complete resection of histologically node-negative esophageal cancer. Surg Today 2007;37:1047–52.
6. Law S Y, Fok M, Wong J. Risk analysis in resection of squamous cell carcinoma of the esophagus. World J Surg 1994;18:339–46.
7. Ferguson MK, Martin TR, Reeder LB, Liu FY, Sun ZY, Xue H. Mortality after esophagectomy: risk factor analysis. World J Surg 1997;21:599–603.
8. Whooley BP, Law S, Murthy SC, Alexandrou A, Wong J. Analysis of reduced death and complication rates after esophageal resection. Ann Surg 2001;233:338–44.
9. Fagevik Olsen M, Wennberg E, Josefson K, Lönroth H, Lundell L. Randomized clinical study of the prevention of pulmonary complications after thoracoabdominal resection by two different breathing techniques. Br J Surg 2002;89:1228–34.
10. Fan ST, Lau WY, Yip WC, Poon GP, Yeung C, Lam WK, et al. Prediction of postoperative pulmonary complications in oesophagogastric cancer surgery. Br J Surg 1987;74:408–10.
11. Law SY, Fok M, Wong J. Risk analysis in resection of squamous cell carcinoma of the esophagus. World J Surg 1994;18:339–46.
12. Lund O, Kimose HH, Aagaard MT, Hasenkam JM, Erlandsen M. Risk stratification and long-term results after surgical treatment of carcinomas of the thoracic esophagus and cardia. A 25-year retrospective study. J Thorac Cardiovasc Surg 1990;99:200–9.
13. Bartels H, Stein HJ, Siewert JR. Preoperative risk analysis and postoperative mortality of oesophagectomy for resectable oesophageal cancer. Br J Surg 1998;85:840–4.
14. Bosset JF, Gignoux M, Triboulet JP, Tiret E, Mantion G, Elias D, et al. Chemoradiotherapy followed by surgery compared with surgery alone in squamous-cell cancer of the esophagus. N Engl J Med 1997;227:161–7.
15. Avendano CE, Flume PA, Silvesri GA, King LB, Reed CE. Pulmonary complications after esophagectomy. Ann Thorac Surg 2002;73:922–6.
16. Fink U, Stein HJ, Wilke H. Multimodal treatment for squamous cell esophageal cancer. World J Surg 1995;19:198–204.
17. Law S, Wong K, Kwak K, Chu KM, Wong J. Predictive factors for postoperative pulmonary complications and mortality after esophagectomy for cancer. Ann Surg 2004;240:791–800.
18. Kelley ST, Coppola D, Karl RC. Neoadjuvant chemoradiotherapy is not associated with a higher complication rate vs surgery alone in patients undergoing esophagectomy. J Gastrointest Surg 2004;8:227–32.
19. Lin FC, Durkin AE, Ferguson MK. Induction therapy does not increase surgical morbidity after esophagectomy for cancer. Ann Thorac Surg 2004;78:1783–9.
20. Tsutsui S, Morita M, Kuwano H, Matsuda H, Mori M, Okamura S, et al. Influence of preoperative treatment and surgical operation on immune function of patients with esophageal carcinoma. J Surg Oncol 1992;49:176–81.
21. Morita M, Yoshida R, Ikeda K, Egashira A, Oki E, Sadanaga N, et al. Acute lung injury following an esophagectomy for esophageal cancer, with special reference to the clinical factors and cytokine levels of peripheral blood and pleural drainage fluid. Dis Esophagus 2008;21:30–6.
22. Akamoto S, Okano K, Sano T, Yachida S, Izuishi K, Usuki H, et al. Neutrophil elastase inhibitor (Sivelestat) preserves antitumor immunity and reduces the inflammatory mediators associated with major surgery. Surg Today 2007;37:359–65.
23. Xu J, Zhong Y, Jing D, Wu Z. Preoperative enteral immunonutrition improves postoperative outcome in patients with gastrointestinal cancer. World J Surg 2006;30:1284–9.
24. Laki K, Lóránd L. On the solubility of fibrin clots. Science 1948;108:280.
25. Canonico S. The use of human fibrin glue in the surgical operations. Acta Biomed 2003;74:21–5.
26. Azim K, McManus R, Brophy K, Ryan A, Kelleher D, Reynolds JV. Genetic polymorphisms and the risk of infection following esophagectomy. positive association with TNF-alpha gene –308 genotype. Ann Surg 2007;246:122–8.

Surg Today (2010) 40:1034–1039
DOI 10.1007/s00595-010-4296-y

Original Article

SURGERY TODAY

A Survey of the Effects of Sivelestat Sodium Administration on Patients with Postoperative Respiratory Dysfunction

HIROSHI SAEKI[1], MASARU MORITA[1], NOBORU HARADA[2], NORIFUMI HARIMOTO[3], SHIGEYUKI NAGATA[1], MITSUHIRO MIYAZAKI[3], TADASHI KOGA[4], EIJI OKI[5], YOSHIHIRO KAKEJI[1], and YOSHIHIKO MAEHARA[1]

[1]Department of Surgery and Science, Graduate School of Medical Sciences, Kyushu University, 3-1-1 Maidashi, Higashi-ku, Fukuoka 812-8582, Japan
[2]Fukuoka City Hospital, Fukuoka, Japan
[3]Iizuka Hospital, Iizuka, Japan
[4]Saiseikai Karatsu Hospital, Karatsu, Japan
[5]National Kyushu Cancer Center, Fukuoka, Japan

Abstract

Purpose. To clarify the clinical significance of sivelestat sodium (SIV) administration, we surveyed the status of 40 patients treated with SIV for respiratory dysfunction following surgery.

Methods. The subjects were patients who received SIV administration due to systemic inflammatory response syndrome (SIRS) and respiratory dysfunction (PaO_2/F_IO_2 ratio ≤300 mmHg) after surgery at the Department of Surgery and Science, Kyushu University, and related facilities between April and December 2008.

Results. The most frequent underlying condition was perforation of the digestive tract, followed by cancer of the upper digestive organs. The main causes of SIRS were surgical stress and infection. The mean P/F ratio at the initiation of SIV administration was 185.5 ± 72.0 mmHg. The ratio increased, and the number of SIRS-related factors decreased with time after SIV administration. Sivelestat sodium was administered within 24 h after the onset of respiratory dysfunction in 87.5% of the patients, and the survival rate at 28 days after the initiation of SIV administration was 90.0%.

Conclusion. Our findings suggest that multidisciplinary postoperative management, including the administration of SIV, during the early phase after the onset of respiratory dysfunction leads to improvements in respiratory function and survival.

Key words Surgical stress · Systemic inflammatory response syndrome · PaO_2/F_IO_2 ratio · Postoperative management · Sivelestat sodium

Introduction

Systemic inflammatory response syndrome (SIRS) persists and progresses in some cases due to surgical stress and complications of trauma and infection. Protraction of the inflammatory responses can diminish patient recovery from surgery, and may lead to multiorgan failure (MOF), resulting in death.[1,2] These inflammatory reactions involve activation of various inflammatory cells and cytokine/chemokine production by these cells.[3,4] Inflammatory reactions play an important role as defensive reactions, but organ impairment may be induced when the responses become excessive.[5]

The involvement of neutrophils in postoperative acute lung injury (ALI)/acute respiratory distress syndrome (ARDS) has been attracting increasing attention.[6] Activated neutrophils release neutrophil elastase, which can injure vascular endothelial cells and increase permeability, inducing further neutrophil infiltration.[7] By binding specifically to neutrophil elastase, sivelestat sodium (SIV) inhibits the neutrophil elastase-induced pulmonary vascular endothelial cell injury, stops the increase in pulmonary vascular permeability, and decreases the alveolar epithelial cell injury, resulting in a therapeutic effect that can be useful for the treatment of ALI/ARDS.

In this study, we surveyed the postoperative status of patients who were administered SIV for postoperative respiratory dysfunction following surgery in our department and related facilities. The aim of the study was to clarify the clinical significance of SIV administration for patients with respiratory dysfunction following surgery.

Patients and Methods

The subjects of this study were 51 patients who underwent surgery at the Department of Surgery and Science,

Reprint requests to: H. Saeki
Received: October 6, 2009 / Accepted: February 15, 2010

Graduate School of Medical Science, Kyushu University, and 19 related facilities between April and December 2008, and were treated with SIV after meeting the following two conditions after surgery: (A) two or more of the four items of the SIRS diagnostic criteria — (1) body temperature >38°C or <36°C, (2) heart rate >90 beats/min, (3) respiratory rate >20 times/min or $PaCO_2$ <32 mmHg, (4) white blood cell count >12 000/μl or <4000/μl or band cells >10%; and (B) a decreased PaO_2/F_IO_2 (P/F ratio) (P/F ratio ≤300 mmHg). Sivelestat sodium was administered intravenously at a rate of 0.2 mg/kg per hour. Out of the 51 patients, 11 had experienced respiratory dysfunction prior to surgery due to their comorbidities. In order to focus on postoperative respiratory dysfunction, these 11 patients were excluded from the analysis.

Physicians filled in a survey form consisting of the following items: patient background (sex, age, underlying disease, surgical division [emergency/scheduled], cause of SIRS [infection, surgical stress, pancreatitis, other], inflammatory markers, number of organs with failure), respiratory function/management, treatment, respiratory function (P/F ratio), chest X-ray score (the number of infiltrated lung quadrants[8]), time-course number of SIRS-positive items, duration of SIRS (days), duration of artificial respiratory management, and outcome after 28 days. Organ failure was judged based on the method reported by Tamakuma et al.[9] (Table 1).

Data are presented as mean ± standard deviation. For statistical analysis, Fisher's exact test, the unpaired *t*-test, the Wilcoxon signed-rank test, and the Cochran–Armitage trend test were employed, and $P < 0.05$ was regarded as significant.

Table 1. Diagnostic criteria for organ failure

Impaired organ	Diagnostic criteria
Heart	Reduced blood pressure (<100 mmHg) The circulating blood volume is normal, and no response to the normal dose of inotropic agents is noted
Liver	Serum bilirubin >5 mg/dl or ALT >200 U
Kidney	BUN >50 mg/dl or serum creatinine >3 mg/dl
Intestine	Intestinal hemorrhage requiring transfusion
Central nervous system	2 digits or higher on the Japan Coma Scale (3-3-9-step system)
Blood coagulation system	DIC based on the criteria established by the Ministry of Health, Labor and Welfare

ALT, alanine aminotransferase; BUN, blood urea nitrogen; DIC, disseminated intravascular coagulation

Results

Background of Patients

The background of the patients is shown in Table 2. Male patients accounted for 70.0% of the subjects, and the mean age of all patients was 67.1 years. Perforation of the digestive tract was the most frequent underlying disease, and was present in 10 patients (25.0%), followed by cancer of the upper digestive organs in 9 patients (22.5%). Half of the cases underwent emergency surgery. Surgical stress was the most frequent cause of SIRS, occurring in 26 patients (65.0%), followed by infection in 18 patients (45.0%). The number of organs with failure (other than the lungs) was 0 or 1 in 67.5% of the cases.

The respiratory function/management at the initiation of SIV administration is shown in Table 3. The P/F ratio was 200–300 mmHg in 18 cases (45.0%), 100–200 mmHg in 14 (35.0%), and 100 mmHg or lower in 8 (20.0%). On chest X-ray examination, infiltration was noted in 30 cases (75.0%). Regarding the respiratory management method, invasive positive pressure ventilation was employed in 36 patients (90.0%) and noninvasive positive pressure ventilation was used in the other 4 patients (10.0%).

Treatment

The postoperative treatments are shown in Table 4. Drugs administered concomitantly were antimicrobial agents in 39 patients (97.5%), protease inhibitors in 18 (45.0%), diuretics in 14 (35.0%), and steroids in 13 (32.5%). Hemocatharsis by endotoxin adsorption was performed in 3 patients (7.5%). Sivelestat sodium was administered within 24 h after the onset of SIRS in 29 cases (72.5%), within 24 h after the initiation of respiratory management in 29 (72.5%), and within 24 h after the occurrence of respiratory dysfunction in 35 (87.5%).

Changes in the P/F Ratio, Chest X-Ray Score, and Number of SIRS-Positive Items

The changes in the P/F ratio, chest X-ray score, and number of positive items on the SIRS list are shown in Fig. 1. The P/F ratio significantly improved with time after the initiation of SIV administration. The number of positive items on the SIRS checklist also significantly decreased after the initiation of SIV administration.

Duration of SIRS, Duration of Artificial Respiratory Management, and Outcome After 28 Days

The duration of SIRS was 6.7 ± 6.9 (range 1–35) days, and that of artificial respiratory management was 9.1 ±